AD_____

Award Number: DAMD17-03-1-0095

TITLE: Molecular Engineering of Vector-Based Oncolytic and Imaging Approaches for Advanced Prostate Cancer

PRINCIPAL INVESTIGATOR: Lily Wu, Ph.D.

CONTRACTING ORGANIZATION: University of California, Los Angeles
Los Angeles, California 90095-1406

REPORT DATE: February 2005

TYPE OF REPORT: Annual

PREPARED FOR: U.S. Army Medical Research and Materiel Command
Fort Detrick, Maryland 21702-5012

DISTRIBUTION STATEMENT: Approved for Public Release;
Distribution Unlimited

The views, opinions and/or findings contained in this report are those of the author(s) and should not be construed as an official Department of the Army position, policy or decision unless so designated by other documentation.

20050826 060

REPORT DOCUMENTATION PAGE

Form Approved
OMB No. 074-0188

Public reporting burden for this collection of information is estimated to average 1 hour per response, including the time for reviewing instructions, searching existing data sources, gathering and maintaining the data needed, and completing and reviewing this collection of information. Send comments regarding this burden estimate or any other aspect of this collection of information, including suggestions for reducing this burden to Washington Headquarters Services, Directorate for Information Operations and Reports, 1215 Jefferson Davis Highway, Suite 1204, Arlington, VA 22202-4302, and to the Office of Management and Budget, Paperwork Reduction Project (0704-0188), Washington, DC 20503

1. AGENCY USE ONLY (Leave blank)	2. REPORT DATE	3. REPORT TYPE AND DATES COVERED
	February 2005	Annual (1 Feb 2004 - 31 Jan 2005)

4. TITLE AND SUBTITLE
Molecular Engineering of Vector-Based Oncolytic and Imaging Approaches for Advanced Prostate Cancer

5. FUNDING NUMBERS
DAMD17-03-1-0095

6. AUTHOR(S)
Lily Wu, Ph.D.

7. PERFORMING ORGANIZATION NAME(S) AND ADDRESS(ES)
University of California, Los Angeles
Los Angeles, California 90095-1406

E-Mail: lwu@mednet.ucla.edu

8. PERFORMING ORGANIZATION REPORT NUMBER

9. SPONSORING / MONITORING AGENCY NAME(S) AND ADDRESS(ES)
U.S. Army Medical Research and Materiel Command
Fort Detrick, Maryland 21702-5012

10. SPONSORING / MONITORING AGENCY REPORT NUMBER

11. SUPPLEMENTARY NOTES

12a. DISTRIBUTION / AVAILABILITY STATEMENT
Approved for Public Release; Distribution Unlimited

12b. DISTRIBUTION CODE

13. ABSTRACT (Maximum 200 Words)

Hormone refractory and metastatic prostate cancer are not well understood. Better animal models, diagnostic and treatment modalities are sorely needed for these advanced stages of disease. We have coupled non-invasive optical imaging to develop metastatic prostate cancer animal models, and vector-based diagnostic and therapeutic approaches. A highly potent and prostate-specific transcriptional regulatory system (TSTA) has been utilized to restrict the expression of our adenoviral vector specifically to prostate or prostate cancer cells. In the diagnostic approach, this TSTA system will be applied to express imaging reporter gene. Alternatively, the TSTA system will be applied to regulate the expression of viral replication proteins in the therapeutic approach. In doing so, the viral amplification and cell lysis will be directed in a prostate-specific manner. To date, the progress of this project is according to the proposed plan as the feasibility and the functionality of the prostate-targeted oncolytic system was demonstrated. Interestingly, during our investigation, we have developed several metastatic human prostate tumor models. The cancer dissemination process in these models can be easily monitored by non-invasive imaging. These metastatic animal models will be the bases for us to investigate the efficacy of our diagnostic and oncolytic therapeutic viral vectors.

14. SUBJECT TERMS
Metastasis, oncolytic adenovirus, gene therapy, imaging

15. NUMBER OF PAGES
40

16. PRICE CODE

17. SECURITY CLASSIFICATION OF REPORT	18. SECURITY CLASSIFICATION OF THIS PAGE	19. SECURITY CLASSIFICATION OF ABSTRACT	20. LIMITATION OF ABSTRACT
Unclassified	Unclassified	Unclassified	Unlimited

Table of Contents

Introduction:

The scope of this project is to develop adenoviral vectors that are capable of mediating gene expression specifically in prostate and prostate cancer cells. We propose to incorporate a highly potent and specific two-step transcriptional amplification (TSTA) system to mediate prostate-targeted gene expression in our vectors. In diagnostic applications, this targeted vector will be utilized to express optical reporter luciferase gene. The hypothesis is that administration of this imaging reporter virus could illuminate prostate metastatic cells in living animals. Our intention was to extend this prostate-specific molecular imaging approach to the high-energy radionuclide Positron Emission Tomography (PET) such that future clinical diagnostic applications can be developed. In a second therapeutic approach, the TSTA system is employed to regulate viral replication, which leads to specific lysis of prostate tumor cells. Creation of consistent and easy to follow metastatic prostate cancer models will be very useful towards the evaluation of the proposed vector-based diagnostic and therapeutic approaches.

Body:

Task 1A: Determine sensitivity of vector-based imaging.

Findings relevant to this task were reported in two manuscripts.

1) Sato M, Johnson M, Zhang L, Gambhir SS, Carey M, Wu L. Functionality of Androgen Receptor-based Gene Expression Imaging in Hormone Refractory Prostate Cancer. 2005 Clinical Cancer Research, in press.
2) Johnson M, Sato M, Burton J, Gambhir SS, Carey M, Wu L. Prostate Cancer-Targeted Suicide Gene Therapy Achieved Effective Tumor Destruction While Safeguarding Against Systemic Toxicity. Submitted.

The results from these two manuscripts concluded that the prostate-specific TSTA adenoviral vector can produce robust PET imaging signals in androgen-independent tumors (Figure 1) and mediate targeted cytotoxic effects in prostate tumors. As PET imaging is a clinical relevant imaging modality, these results support the translatability of our approach to future clinical diagnostic applications.

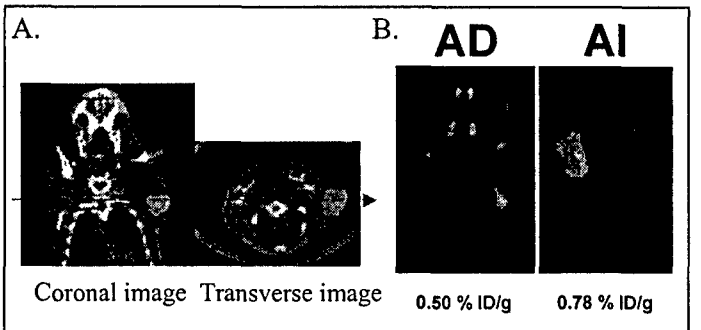

Figure 1. PET imaging of prostate tumors mediated by TSTA vector. The prostate-specific TSTA adenoviral vector that expresses HSV thymidine kinase (sr39tk) gene produced robust 3-D PET signals in the tumor after intratumoral injection of 10exp9 infectious units of vector (A). Signal is higher in AI than AD tumors (B).

Task 1B: To generate optically marked metastatic prostate tumor models to allow detection by prostate-targeted imaging vector.

Significant progress was made in this task (unpublished data). Metastatic characteristics of several human prostate cancer xenografts (LAPC series,1) were determined. By marking tumor cells by transducing with a firefly luciferase-expressing lentiviral vector, we were able to monitor the metastatic events by optical CCD imaging (Adams et al. Nat Med 8:891, 2002). We observed that the human LAPC-

4 prostate cancer xenograft, originally derived from lymph node metastases, exhibit higher metastatic potential in SCID mice than the LAPC-9, which was derived from a bone metastatic lesion (Figure 2). Analyses and comparison of gene expression in these two models by quantitative real-time RT-PCR revealed that expression of pro-lymphangiogenic growth factor VEGF-C was 70-fold elevated in LAPC-4 over LAPC-9 tumors.

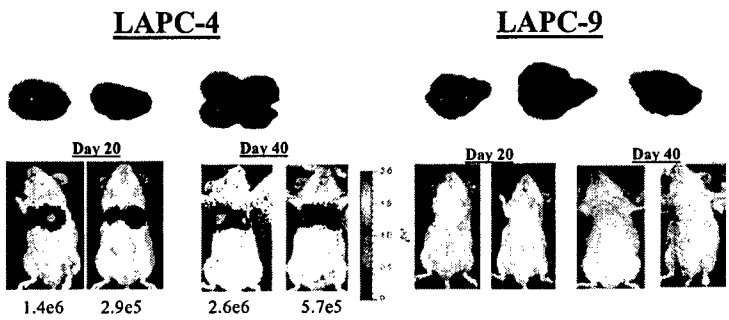

Figure 2. Two prostate-tumors exhibit distinct metastatic potential and gross vascularity. Optically labeled tumors were established subcutaneously, resected at 1cm dia and metastatic events were monitored by repetitive optical imaging. LAPC-4 tumor exhibited increased metastasis as imaged on the specified dates.

To extend the investigation on the contribution of tumor lymphangiogenesis to metastasis, we employed a lentiviral-mediated approach to induce over-expression of angiogenic and lymphangiogenic growth factors. Extensive animal experimentations are still underway at this time. Preliminary data indicated that overexpression of VEGF-C can induce lymph node metastasis even in tumor with low metastatic potential such as LAPC-9 (Figure 3).

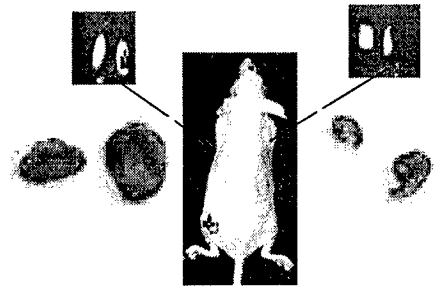

Figure 3. Overexpression of VEGF-C in low metastatic tumor. LAPC-9 tumor cells were transduced with a CMV-VEGF-C ires GFP lentivirus. Metastases to ipsilateral axillary lymph nodes in the LAPC-9/VEGF-C tumor bearing animals but not the control group. The infiltrated lymph nodes were enlarged and exhibited positive optical signals.

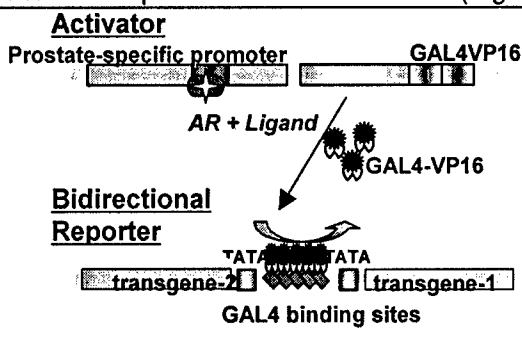

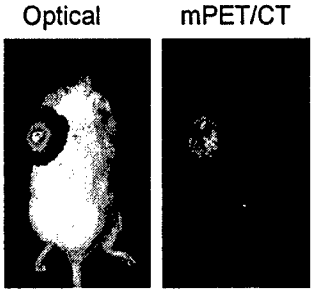

Figure 4. Bidirectional TSTA expression. Injection of the FL (transgene 1)/ TK (transgene 2) virus with the activator AdBC-VP2 virus resulted in simultaneous expression of both genes (i.e. both optical and PET imaging signals) in the same tumor.

Task 2A: Generation of therapeutic oncolytic adenovirus.

In the oncolytic adenovirus under development, we will employ the TSTA prostate-specific expression system to drive viral E1A and E1B protein in a bi-directional scheme (Figure 4, 5). To confirm that the bi-direction expression of two genes can be regulated by the centrally located Gal4-VP16 activators, we have created a virus that expresses firefly luciferase (FL) and herpes simplex thymidine kinase (TK) gene in divergent orientation (Figure 4). Co-infection of this bi-directional

reporter virus with a Gal4-VP16 activator-expressing virus (AdBC-VP2, 3) resulted in expression of both FL and TK proteins, which can be detected by optical and PET imaging simultaneously (Figure 4). Our group has shown that this bi-directional TSTA expression system was feasible in DNA a plasmid transfection study (Ray et al. below).

Applying this bi-directional expression approach, we demonstrated that in the designed oncolytic viral constructs both E1A and E1B gene were expressed in an androgen regulated manner. Moreover, viral replication can be induced specifically (Figure 5). These results supported that the feasibility of our oncolytic virus to mediate viral replication and, hence, tumor cell lysis in a prostate-specific manner. The examination of the therapeutic activity of the oncolytic virus in tumor models will be underway shortly.

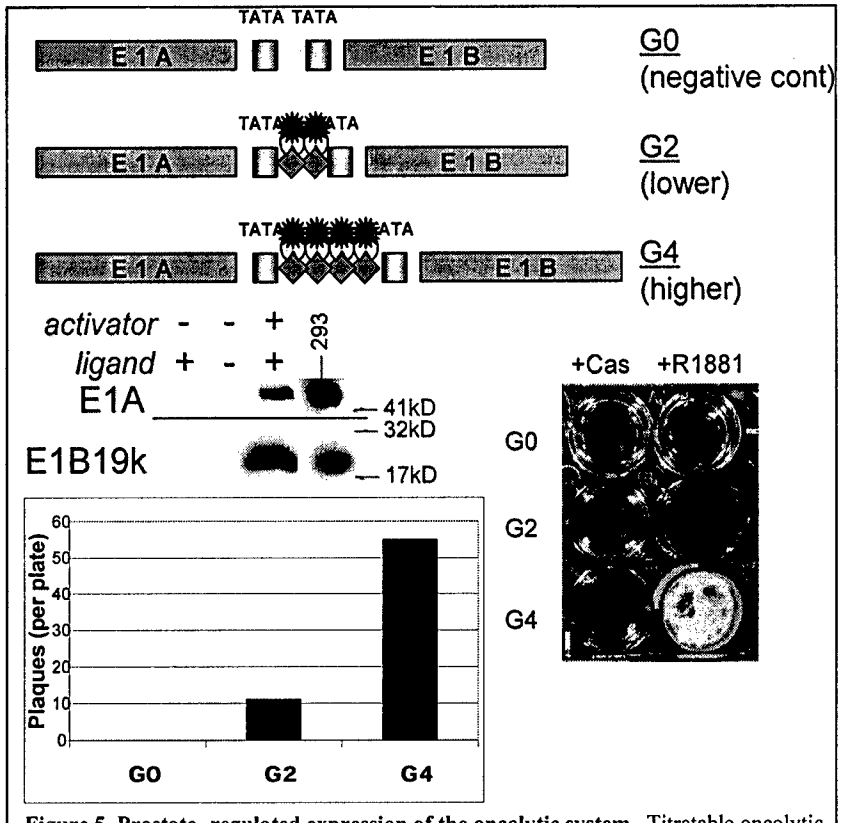

Figure 5. Prostate- regulated expression of the oncolytic system. Titratable oncolytic constructs with 0 to 4 binding sites of Gal4 activators (G0, G2, and G4, top diagram) were created. E1A and E1B protein expression was regulated by the ligand (middle panel, result of G4 shown). The regulated expression of E1 proteins induced the replication of a luciferase-expressing virus, which could be measured by optical imaging of the infected cells (lower right panel) and plaque formation (lower left panel). The gradation of replication was controlled in a Gal4 site responsive manner.

Key Research Accomplishments:

1. An adenoviral vector containing the prostate-targeted TSTA system is able to mediate robust PET imaging in advanced androgen independent prostate tumor.
2. Many metastatic prostate tumor models are being established. Detailed characterization of the biology of metastatic process and tumor vasculatures would enable us to better delineate the path of metastasis and design optimal diagnostic imaging strategies to detect metastases.
3. Functionality of the bi-directional TSTA mediated simultaneous expression of two genes was established.
4. Feasibility of the bi-directional oncolytic virus was also supported.

Reportable Outcomes:

Manuscripts:

1) *Ray S, Paulmurugan R, Hildebrandt I, Iyer M, Wu L, Carey M, Gambhir SS. Novel bidirectional vector strategy for amplification of therapeutic and reporter gene expression. Hu Gene Ther. 2004 15:681-90. (enclosed)*
2) *Sato M, Johnson M, Zhang L, Gambhir SS, Carey M, Wu L. Functionality of Androgen Receptor-based Gene Expression Imaging in Hormone Refractory Prostate Cancer. Clin Can Res 2005, in press. (enclosed)*
3) *Johnson M, Sato M, Burton J, Gambhir SS, Carey M, Wu L. Prostate Cancer-Targeted Suicide Gene Therapy Achieved Effective Tumor Destruction While Safeguarding Against Systemic Toxicity. Submitted.*

Abstracts:

1) *Sato M, Johnson M, Zhang L, Gambhir SS, Carey M and Wu L. Development of Prostate Specific Oncolytic Adenovirus Utilizing Bidirectional TSTA System. AACR special meeting-Basic, Translational, and Clinical Advances in Prostate Cancer at Bonita Springs, FL. 11/2004, travel award.*
2) *Makoto Sato, Mai Johnson, Michael Carey, Sanjiv Gambhir and Lily Wu. "Development of Prostate Specific Oncolytic Adenovirus Utilizing the Bidirectional TSTA System". Academy of Molecular Imaging annual meeting, March 20-23, 2005, Orlando Florida, supported travel award.*
3) *Johnson M, Sato M, Burton J, Gambhir SS, Carey M, Wu L. "Prostate Cancer-Targeted Suicide Gene Therapy Achieved Effective Tumor Destruction While Safeguarding Against Systemic Toxicity", Academy of Molecular Imaging annual meeting, March 20-23, 2005, Orlando Florida, supported travel award. .*
4) *Sato M, Johnson M, Zhang L, Gambhir SS, Carey M and Wu L. "Prostate-Specific Oncolytic Adenovirus Based on Bidirectional TSTA System". American Society of Gene Therapy (ASGT) annual meeting at St. Louis, MO. 6/2005.*

Presentations:

1) In vivo Models of Experimental Therapeutics Relevant to Human Cancer, NCI Workship, invited speaker, Frederick, Maryland, April 1, 2004. (Meeting report published in Cancer Res, 2004 64:8478-8480)
2) Lymphangiogenesis and Cancer NCI Workshop, invited speaker, Georgetown, Washington DC, April 21-23, 2004. (Meeting report published in Cancer Res, Cancer Res. 2004 64:9225-9229)
3) Therapeutic Targeting of Human Prostate Cancer Symposium, invited speaker, Tucson, Arizona, May 6-9, 2004.
4) Inter-Prostate SPORE Meeting, Houston, Texas, Jan 30 – Feb 1, 2005, invited speaker.

Conclusions:

We have demonstrated that the TSTA approach can greatly augment prostate-specific gene expression. Imaging and therapeutic TSTA adenoviral vectors mediate targeted gene expression in animal prostate tumor models. The feasibility and functionality of prostate-specific oncolytic adenovirus regulated by the bi-directional TSTA system has been established. We have also generated metastatic prostate cancer models marked with sensitive optical reporter gene. These models will facilitate the investigation of tumor biology and serve as excellent models to investigate our vector-based imaging and oncolytic therapeutic strategy for metastatic disease.

References:

1. Klein, K. A., Reiter, R. E., Redula, J., Moradi, H., Zhu, X. L., Brothman, A. R., Lamb, D. J., Marcelli, M., Belldegrun, A., Witte, O. N., and Sawyers, C. L. Progression of metastatic human prostate cancer to androgen independence in immunodeficient SCID mice, Nat Med. 3: 402-8,1997.
2. Adams JY, Sato M, Johnson M, Berger F, Gambhir S S, Carey M, Iruela-Arispe ML, Wu L. Visualization of Advanced Human Prostate Cancer Lesions in Living Mice by a Targeted Gene Transfer Vector and Optical Imaging. Nat Med, 8:891-7, 2002.
3. Sato M, Johnson M, Zhang L, Zhang B, Le K, Gambhir SS, Carey M and Wu L. Optimization of Adenoviral Vectors to Direct Highly Amplified Prostate-Specific Gene Expression for Imaging and Gene Therapy. Mol Ther, 8: 726-737, 2003.

HUMAN GENE THERAPY 15:681–690 (July 2004)
© Mary Ann Liebert, Inc.

Novel Bidirectional Vector Strategy for Amplification of Therapeutic and Reporter Gene Expression

SUNETRA RAY,[1,4] RAMASAMY PAULMURUGAN,[1] ISABEL HILDEBRANDT,[1] MEERA IYER,[1] LILY WU,[2] MICHAEL CAREY,[3] and SANJIV S. GAMBHIR[1,4–7]

ABSTRACT

Molecular imaging methods have previously been employed to image tissue-specific reporter gene expression by a two-step transcriptional amplification (TSTA) strategy. We have now developed a new bidirectional vector system, based on the TSTA strategy, that can simultaneously amplify expression for both a target gene and a reporter gene, using a relatively weak promoter. We used the synthetic *Renilla* luciferase (*hrl*) and firefly luciferase (*fl*) reporter genes to validate the system in cell cultures and in living mice. When mammalian cells were transiently cotransfected with the GAL4-responsive bidirectional reporter vector and various doses of the activator plasmid encoding the GAL4-VP16 fusion protein, pSV40-GAL4-VP16, a high correlation (r^2 = 0.95) was observed between the expression levels of both reporter genes. Good correlations (r^2 = 0.82 and 0.66, respectively) were also observed *in vivo* when the transiently transfected cells were implanted subcutaneously in mice or when the two plasmids were delivered by hydrodynamic injection and imaged. This work establishes a novel bidirectional vector approach utilizing the TSTA strategy for both target and reporter gene amplification. This validated approach should prove useful for the development of novel gene therapy vectors, as well as for transgenic models, allowing noninvasive imaging for indirect monitoring and amplification of target gene expression.

OVERVIEW SUMMARY

Tissue-specific promoters frequently used for tissue-specific delivery of therapeutic genes in gene therapy applications are limited by their weak transcriptional ability. To overcome this drawback the two-step transcriptional amplification (TSTA) strategy was designed to enhance the promoter strengths of such weak tissue-specific promoters. Here, we report on the engineering, functional characterization, and *in vivo* application of a bidirectional TSTA system that will allow us to simultaneously amplify the expression of a therapeutic gene and that of a tightly coupled reporter gene. We demonstrate that such a bidirectional TSTA system will also be helpful in quantifying the amplified expression of the therapeutic gene simply by studying the highly correlated expression of the tightly coupled reporter gene.

INTRODUCTION

CONVENTIONAL NONINVASIVE CANCER THERAPY is often hampered by a lack of tumor specificity that frequently culminates in unwanted severe adverse effects, thereby limiting therapeutic doses and rendering the malignant lesions resilient to treatment (Nettelbeck *et al.*, 1998, 2000). Gene therapy continues to be investigated as a potential alternative to the drawbacks of traditional cancer therapy. Thus the goal is to achieve high levels of transcription of a transgene in the desired cell

[1]Crump Institute for Molecular Imaging, UCLA School of Medicine, Los Angeles, CA 90095.
[2]Department of Urology, UCLA School of Medicine, Los Angeles, CA 90095.
[3]Department of Biological Chemistry, UCLA School of Medicine, Los Angeles, CA 90095.
[4]Department of Molecular and Medical Pharmacology, UCLA School of Medicine, Los Angeles, CA 90095.
[5]UCLA-Jonsson Comprehensive Cancer Center, UCLA School of Medicine, Los Angeles, CA 90095.
[6]Department of Biomathematics, UCLA School of Medicine, Los Angeles, CA 90095.
[7]Department of Radiology, Stanford University School of Medicine, Stanford, CA 94305.

population by the use of cell-specific promoters or regulatory elements. However, a majority of these tissue-specific promoters are also inherently weaker activators of transcription, and even when suitably delivered to the target site, are often unable to achieve therapeutic levels of the protein transcribed from the therapeutic gene (TG). Thus it became imperative to design strategies to enhance promoter strength, while maintaining specificity, of these weak tissue-specific promoters (Nettelbeck *et al.*, 2000).

Several strategies have been successfully implemented so far. These include (1) designing a minimal promoter by eliminating from a natural promoter all the other elements that do not contribute to promoter strength, (2) designing promoters containing activated point mutations, (3) constructing chimeric promoters by combining the transcriptional regulatory elements from different promoters specific for the same tissue, (4) enhancement at the posttranslational level, and (5) using recombinant transcriptional activators (RTAs) that assist in achieving transcriptional amplification (Nettelbeck *et al.*, 2000; Iyer *et al.*, 2001).

The RTA approach, also referred to as the two-step transcriptional amplification (TSTA) approach, has been effectively used to enhance the transcriptional ability of tissue-specific promoters in both cell culture and in living animals. In this approach the promoter drives the production of the potent GAL4-VP16 transcriptional activator, encoded by the "activator" plasmid. This chimeric transcription factor, consisting of the highly potent activation domain of the herpes simplex virus type 1 (HSV1) VP16 immediate-early *trans*-activator fused to the yeast GAL4-DNA-binding domain, in turn acts on a second expression plasmid encoding the reporter/therapeutic proteins through a GAL4-responsive minimal promoter bearing multiple tandem copies of the 17-bp GAL4-binding sites (G5) placed upstream from the genes of interest. Iyer *et al.* (2001) and Zhang *et al.* (2002) used the TSTA strategy, in combination with positron emission tomography (PET) and optical methods, to amplify and image the expression of reporter genes—mutant HSV1 thymidine kinase (HSV1-sr39*tk*) and firefly luciferase (*fl*), respectively—in living animals. These studies validated the ability of the TSTA system to enhance the transcriptional ability of a weak tissue-specific promoter, the prostate-specific antigen enhancer/promoter (PSE). The system was also valuable in demonstrating androgen-responsive activity in prostate cancer cells (Iyer *et al.*, 2001; Zhang *et al.*, 2002). Another study used a similar approach to achieve tumor-specific amplification of gene expression from a novel suicide gene therapy adenoviral vector driven by a weak tissue-specific CEA promoter (Qiao *et al.*, 2002).

Precise localization and quantitative assessment of the level of gene expression are highly desirable for the evaluation of gene therapy trials (Massoud and Gambhir, 2003). A number of methodologies can be employed to image reporter genes in living subjects. Among them PET, single-photon emission computed tomography (SPECT), magnetic resonance imaging (MRI), and optical imaging are well standardized and can be extensively used to study reporter gene expression repeatedly and noninvasively (Wang, 2001; Weber *et al.*, 2001; Massoud and Gambhir, 2003; Ray *et al.*, 2003). Although PET has good spatial resolution, high sensitivity, and tomographic capabilities, it is limited by higher cost and the risk of radioactive exposure. In contrast, optical imaging techniques (fluorescence and bioluminescence) can be a low-cost and quick alternative for real-time analysis of gene expression in small animals with just transiently transfected cells (Zhang *et al.*, 1999; Contag and Bachmann, 2002; Contag and Ross, 2002; Negrin *et al.*, 2002; Ray *et al.*, 2003). Our laboratory has successfully used both *fl* and synthetic *Renilla* luciferase (*hrl*) as bioluminescence optical reporter genes to study gene expression in small animals. We have also reported that both *fl* and *hrl* can be imaged in the same animal and that they present different light production kinetics without any substrate cross-reactivity (Bhaumik and Gambhir, 2002a,b).

Gene expression can be imaged directly if the transgene or therapeutic gene (TG) is also an imaging reporter gene (RG), for example, HSV1-*tk* or the mutant thymidine kinase (HSV1-sr39*tk*) gene, whose protein product HSV1 thymidine kinase (HSV1-TK/SR39TK) can trap various radiolabeled substrates in cells and hence can be detected by PET/SPECT (Gambhir *et al.*, 1998, 2000; Eckelman *et al.*, 2000; Lammertsma, 2001; Luker and Piwnica-Worms, 2001; Sharma *et al.*, 2002; Blake *et al.*, 2003; Massoud and Gambhir, 2003). Unfortunately, most therapeutic transgenes lack the appropriate ligands or substrates that can be radiolabeled and used to generate images that define the magnitude of gene expression. Thus general strategies have been developed and validated to link the expression of the TG to a PET or optical RG and to track *in vivo* expression of the TG indirectly by imaging the RG. Linking the expression of the TG to the RG can be achieved through a variety of different molecular constructs (Ray *et al.*, 2001; Sundaresan and Gambhir, 2002). One approach is to clone both genes, one immediately following the other (with or without a short spacer) (Ray *et al.*, 2003), downstream of a single promoter. A single mRNA strand carrying the coding regions of both genes will be transcribed from this construct and will encode a fusion protein. This approach requires that the function of the reporter protein or the therapeutic protein not be significantly compromised as a result of the fusion. A second approach is to place both genes in different locations in the same vector, each downstream of identical but independent promoters (Ray *et al.*, 2001; Sun *et al.*, 2001; Yaghoubi *et al.*, 2001). Because the promoters are identical, theoretically, the two separate mRNAs and proteins that are produced should be correlated. A simpler method is to coadminister two identical vectors, one carrying the TG and the other the RG. Our laboratory has demonstrated that it is possible to macroscopically correlate the expression of two genes by regulating their transcription with the same promoter, but delivering them on separate adenoviral vectors (Yaghoubi *et al.*, 2001). An additional method for transcriptional linking of the TG with the RG is by the use of a bicistronic vector, containing an internal ribosomal entry site (IRES). In this case both genes are transcribed into a single mRNA from the same promoter but are translated into two different proteins with the help of the IRES sequences (Ray *et al.*, 2001). Yu *et al.* constructed such a vector in which the dopamine type 2 receptor (*D2R*) RG was placed upstream and the HSV1-sr39*tk* RG was placed downstream of the encephalomyocarditis (EMCV) IRES. Transcription of both genes was directed by a cytomegalovirus (CMV) promoter (Yu *et al.*, 2000). C6 glioma cells stably transfected with the vector expressed both genes with high correlation. However, a drawback of the IRES system is the attenuation of expression of the gene downstream of the IRES sequence. Chappell *et al.* identified a novel IRES within the mRNA of the homeodomain protein Gtx that produced 60-fold higher activity compared with the EMCV–IRES in cell cultures (Chappell *et al.*, 2000). Our

laboratory has used the Gtx–IRES to produce novel gene therapy vectors to overcome the attenuation of the downstream gene (Wang, 2001).

Earlier, Baron *et al.* (1995) constructed a tetracycline-inducible novel vector system in which a single bidirectional tetracycline-inducible promoter can be used to control the expression of any pair of genes in a correlated, dose-dependent manner. We applied this bidirectional strategy and obtained highly correlated expression of two PET reporter genes in living subjects (Sun *et al.*, 2001).

In the current study, our objective was to develop a new bidirectional vector system, based on the TSTA/RTA model, that can amplify the expression of both a TG and a RG simultaneously (Fig. 1). This system should help in determining the spatial location(s) and level of expression of the target gene with the help of the highly correlated expression of the tightly coupled reporter gene, which can be imaged noninvasively. The system consists of two components: (1) an activator plasmid encoding the GAL4-VP16 *trans*-activator protein and (2) a reporter plasmid carrying two optical reporter genes in opposite orientations flanking a bidirectional GAL4-responsive promoter system. One or both of the reporter genes can be changed to a therapeutic gene of interest. Our results show that two optical reporter genes encoding firefly luciferase (FL) and synthetic *Renilla* luciferase (hRL) are indeed coregulated in a quantitative manner by means of this strategy, both in cell culture as well as in living animals imaged with an optical system.

MATERIALS AND METHODS

Chemicals

Dulbecco's modified Eagle's medium (DMEM) was purchased from GIBCO-BRL (Grand Island, NY). A luciferase assay kit was purchased from Promega (Madison, WI). D-Luciferin potassium salt, a substrate for FL, was obtained from

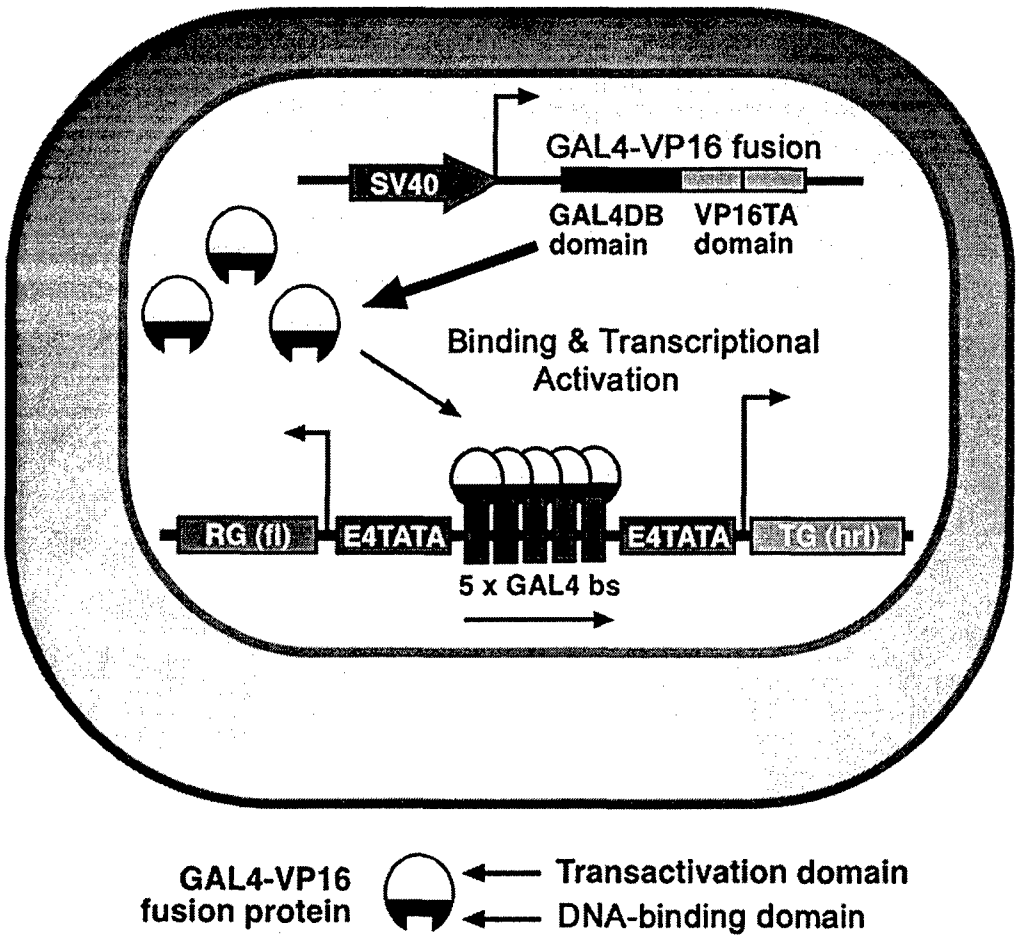

FIG. 1. Schematic diagram of the bidirectional system. The first construct is the activator plasmid pSV40-GAL4-VP16 (referred to as VP16 in text), responsible for driving expression of the GAL4-VP16 fusion protein under the control of the constitutive SV40 promoter. GAL4-VP16 consists of the N-terminal portion of the VP16 activation domain (amino acids 413–454) fused to the GAL4 DNA-binding domain (amino acids 1–147). The second construct depicts the design of the bidirectional reporter plasmid (*fl*-G5-*hrl*). The genes are under the control of the GAL4-responsive bidirectional minimal promoter. One of two genes can be a target gene (TG) (*hrl*) while the other can be a reporter gene (RG) (*fl*). The GAL4-VP16 fusion protein can potentially lead to amplification of both TG and RG simultaneously, with the tightly coupled reporter gene providing indirect quantitation and imaging locations of the TG.

Xenogen (Alameda, CA). Coelenterazine, the substrate for hRL, was purchased from Biotium (Hayward, CA).

Cell culture

N_{2a} cells (mouse neuroblastoma), 293T cells (human kidney), and HeLa cells (human cervical carcinoma) were grown in DMEM high-glucose supplemented with 10% fetal bovine serum (FBS) and 1% penicillin–streptomycin solution.

Construction of plasmids/vectors

The activator plasmid pSP72-SV40-GAL4-VP16 was constructed as described earlier (Iyer *et al.*, 2001). Multiple steps of cloning and polymerase chain reaction (PCR) amplifications were employed to construct the bidirectional *fl*-G5-*hrl* (reporter) plasmid that contains a GAL4-responsive bidirectional promoter in the center connecting the forward (*hrl*) and backward (*fl*) genes. The promoter consists of five GAL4-binding sites (17 bp each) flanked on each side by two TATA box-containing minimal promoters from the adenoviral E4 gene (E4TATA) as described previously (Iyer *et al.*, 2001). The *hrl* gene excised from the pCMV-hrl plasmid (Promega) was first inserted between the *Nhe*I and *Not*I sites in multiple cloning site I (MCSI) of the PBIL vector obtained from BD Biosciences Clontech (Palo Alto, CA). The G5-E4T cassette was PCR amplified from the G5E4T-fl vector (Iyer *et al.*, 2001), using a 5′-end primer with an *Stu*I site attached (AATTAGGCCTAATTCTCGAGATTTAGGTGACACTATAGAAT) and a 3′-end primer with an *Nhe*I site attached (AATTGCTAGCACACCACTCGACACGGCACC). The 5′-end primer also encoded a unique *Xho*I site just following the *Stu*I site. The PCR fragment was subsequently digested with *Stu*I and *Nhe*I and cloned into the PBIL vector. The second E4TATA minimal promoter was then inserted in the (−) strand preceding the *fl* gene in the vector. The E4TATA sequence was PCR amplified from the pSP72-E4TATA-CAT plasmid (Iyer *et al.*, 2001), using an upstream primer with an *Xho*I site (AATTCTCGAGGGATCCCCAGTCCTATATATACT) and a 3′-end primer with an *Sac*II site (AATTCCGCGGACACCACTCGACACGGCACC). The E4T-G5-E4T cassette completely replaced the TRE promoter element in the original PBIL vector.

For the sake of convenience the bidirectional reporter template with *fl* and *hrl* is abbreviated as *fl*-G5-*hrl*, the *trans*-activator plasmid pSV40-GAL4-VP16 is VP16, and the unidirectional TSTA system is G5fl.

Cell transfections and enzyme assays

Cells were plated in 12-well plates in DMEM containing 10% FBS. Transient transfections were performed 36 hr later with Superfect transfection reagent. Each transfection mix contained different dose combinations of the reporter plasmid *fl*-G5-*hrl* and the activator plasmid VP16. After 24 hr of incubation the cells were harvested and the cell lysate was used for enzyme assays.

Luciferase assays

All bioluminescence assays were performed in a TD 20/20 luminometer (Turner Designs, Sunnyvale, CA) with an integration time of 10 sec. The protein content of the cell lysates was determined with a Bio-Rad protein assay system (Bio-Rad, Hercules, CA) in a DU-50 spectrophotometer (Beckman Coulter, Fullerton, CA) and the luminescence results are reported as relative light units (RLU) per microgram of protein.

FL assays were carried on with a luciferase assay kit from Promega. *Renilla* luciferase assays were performed as described previously (Bhaumik and Gambhir, 2002a).

Preparation of coelenterazine and D-luciferin

A stock solution of coelenterazine in methanol (2 mg/ml) was further diluted with phosphate-buffered saline (PBS). A 15-mg/ml stock solution of D-luciferin in PBS was filtered through 0.22-μm pore size filters before use.

Imaging FL and hRL bioluminescence in living animals

All handling of animals was performed in accordance with University of California, Los Angeles and Animal Research Committee guidelines. N_{2a} cells were transiently cotransfected with *fl*-G5-*hrl* and various doses of VP16. Cells were harvested 24 hr after transfection and resuspended in PBS. Adult male nude mice were injected with 1×10^6 cells in four different sites subcutaneously, each site representing cells transfected with a particular dose of the activator plasmid, 30 min before imaging. The naked DNA experiments were performed in male CD-1 mice more than 6 weeks of age. Both plasmids, in different proportions (as described in Results), were mixed thoroughly with 2 ml of PBS and kept in ice. The whole volume was then rapidly (within 2–3 sec) injected (hydrodynamic injection) into the tail vein of each animal. Animals were subjected to bioluminescence imaging 6 and 24 hr postinjection.

For imaging *hrl* gene expression 100 μl of the coelenterazine (20 μg for xenograft studies and 40 μg for naked DNA experiments) was injected via the tail vein approximately 10 sec before imaging, whereas to image *fl* gene expression 200 μl of D-luciferin (3 mg) was injected intraperitoneally 10 min before imaging. All mice were imaged with a cooled charge-coupled device (CCD) camera (IVIS; Xenogen) and photons emitted from cells implanted in the mice were collected and integrated for a period of 1 min. Images were obtained with Living Image software (Xenogen) and IGOR image analysis software (Wavemetrics, Lake Oswego, OR). Imaging was continued until the hRL signal dropped beyond detectable limits (~2 hr). The animals were then injected intraperitoneally with 200 μl of D-luciferin stock solution and each animal was imaged for 15 min, with 1 min of acquisition each time.

For quantification, regions of interest (ROIs) were drawn over the sites of implantation and maximum photons/sec/cm^2/steradian was obtained.

Statistical testing

Linear regression analysis was performed to assess the linear relationship between two variables. The strength of correlation between them was quantified in terms of the square of the Pearson correlation coefficient (r^2). The significance of correlation was obtained by performing the Student t test against the null hypothesis that the correlation coefficient (r) is zero. Values of $p < 0.05$ were considered statistically significant. All cell culture and mouse group comparisons were performed with a Student t test. Values of $p \leq 0.05$ were considered statistically significant.

RESULTS

A GAL4-responsive bidirectional strategy can amplify the expression of two independent reporter genes in transiently transfected cells

To determine, in cell culture, whether this novel strategy has the potential to amplify the expression of both reporter genes simultaneously, N_{2a} cells were transiently cotransfected in 12-well plates with the activator (VP16) and the reporter (*fl*-G5-*hrl*) plasmids in a 1:1 ratio and the cell lysates were assayed 24 hr after transfection. Robust expressions of both reporter genes were obtained in the presence of the GAL4-VP16 fusion protein compared to cells transfected with the same amount of reporter plasmid alone (Fig. 2A and B). Firefly luciferase protein activity is about 2000-fold higher than in mock-transfected cells and cells transfected with activator plasmid only, and about 300-fold higher than in cells transfected with only the reporter plasmid. Similarly, there is a 500- and 600-fold gain in expression of the *hrl* gene in cells cotransfected with both plasmids compared with cells carrying only the activator plasmid or the reporter plasmid, respectively, and a 700-fold gain compared with mock-transfected cells. This result illustrates, primarily, that this novel vector will allow us to drive the expression of both genes simultaneously in the presence of GAL4-VP16. When CMV-*hrl* is compared with the bidirectional system, there is 2-fold lower hRL activity in the case of the latter ($p = 0.005$). However, when compared with CMV-*fl*, *fl* expression is about 3- to 4-fold lower ($p = 0.003$) in the case of the bidirectional system. A comparison of *fl* gene activity with the unidirectional TSTA system (G5-*fl*) (Iyer *et al.*, 2001) reveals about a 3- to 4-fold drop with the bidirectional model ($p < 0.01$). To determine whether the results are consistent across cell lines, similar experiments were repeated in other mammalian cell lines (HeLa and 293T). Similar results were obtained in both cell lines, with 293T cells showing the highest expression levels of both genes. These results indicate that the bidirectional system can cause significant amplification in the expression of both genes simultaneously in the presence of the *trans*-activator, and that the results are reproducible across several cell lines.

Linearly increasing levels of fl and hrl expression are observed in N_{2a} cells transfected with increasing doses of activator plasmid when the dose of reporter plasmid is kept constant

To confirm that the levels of expression of the reporter genes increase in accordance with increasing levels of the activator protein GAL4-VP16, we transfected N_{2a} cells with increasing doses of VP16 (0–0.75 μg/well) along with a constant dose of the reporter plasmid (0.5 μg/well). Cells transfected with only the reporter plasmid were used as the control. We observed a linear increase in hRL and FL enzyme activities up to 0.75 μg/well (Fig. 3A and B). Thus within a 0- to 0.75-μg/well dose of the activator plasmid both FL and hRL activities correlate well with the amount of the activator protein ($r^2 = 0.98$ and 0.90, respectively).

The bidirectional reporter system produces highly correlated expression of two independent reporter genes in cell culture studies

To determine in cell culture whether the expression of a reporter gene can be used to estimate the expression of a linked transgene, using the current strategy, we cotransfected N_{2a} (0–0.75 μg/well), HeLa (0–0.75 μg/well), and 293T (0–0.8 μg/well) cells with various doses of the activator plasmid and a constant dose (0.5 μg/well) of the reporter plasmid. After 24 hr of transfection the cell lysates were collected and assayed for FL and hRL enzyme activities. Figure 3C illustrates correlation between the activities of the two luciferases stated as average relative light units (RLU) per microgram of protein. Regression analysis shows high correlation ($r^2 = 0.94$) between the FL and hRL activities in N_{2a} cells. High correlations are also seen in the case of HeLa ($r^2 = 0.98$) and 293T cells ($r^2 = 0.92$) (data not shown).

Expression of both reporter genes increases linearly and in a highly correlated fashion in cells transfected with various doses of the reporter plasmid while keeping the dose of the activator plasmid constant

To see whether the results were reproducible if the dose of the reporter component of the system was changed while keeping the activator component constant, we repeated the transfection studies with multiple doses of the reporter plasmid (0–0.75 μg/well) while the amount of the activator plasmid was kept constant at 0.5 μg/well in N_{2a} cells. The FL and hRL ac-

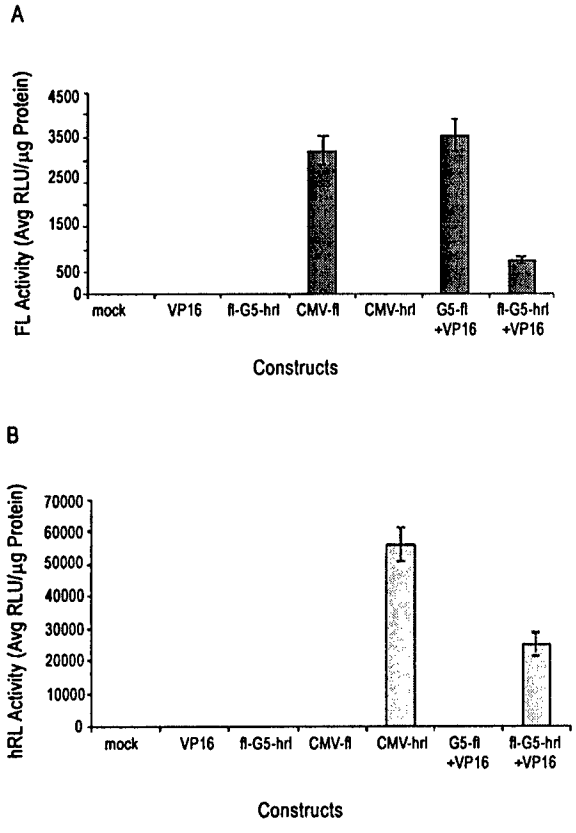

FIG. 2. The bidirectional system mediates simultaneous expression of both *fl* (**A**) and *hrl* (**B**) genes. N_{2a} cells were transiently transfected with water (mock), activator plasmid alone (VP16), reporter plasmid alone (*fl*-G5-*hrl*), CMV-fl, CMV-hrl, Unidirectional *fl* TSTA system (G5fl+VP16), or both reporter and activator (*fl*-G5-*hrl*+VP16). The cells were harvested 24 hr after transfection and assayed for FL and hRL activity. Error bars represent the SEM for triplicate measurements.

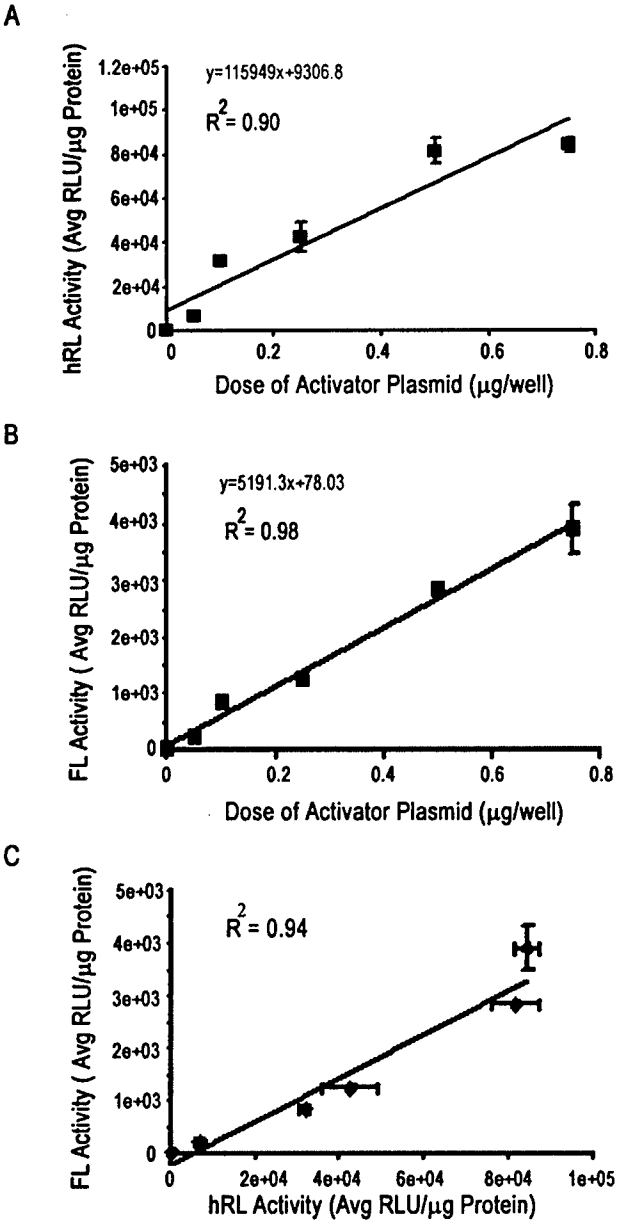

FIG. 3. Linear increase in gene expression with increasing doses of the activator plasmid. (**A**) and (**B**) show the linear increase in expression of the *hrl* and *fl* genes, respectively, as the activator plasmid (VP16) dose is increased from 0 to 0.75 µg/well while the dose of reporter plasmid is maintained at 0.5 µg/well. Seen here are high correlations (r^2 = 0.90 and 0.98 for *hrl* and *fl*, respectively) between the dose of activator plasmid used for transfection and protein activities. The results were obtained 24 hr after transfection in N_{2a} cells. Error bars indicate the SEM for triplicate measurements. (**C**) Correlation between *hrl* and *fl* expression in N_{2a} cells transfected with various doses of VP16 and a constant dose of *fl*-G5-*hrl*. The correlation is r^2 = 0.94.

tivities again increased linearly with increasing doses of the reporter as revealed by regression analysis (Fig. 4A and B) (r^2 = 0.98 and 0.96, respectively). The activities of both genes were also highly correlated (r^2 = 0.99) (Fig. 4C). The results were also reproducible in both HeLa and 293T cells (r^2 = 0.95 and 0.98, respectively), although in the latter case the level of expression was much higher (data not shown).

Amplified expression levels of optical reporter genes fl *and* hrl *can be imaged in individual living animals and are highly correlated*

We next examined whether the GAL4-responsive bidirectional reporter system can regulate expression of both *fl* and *hrl*

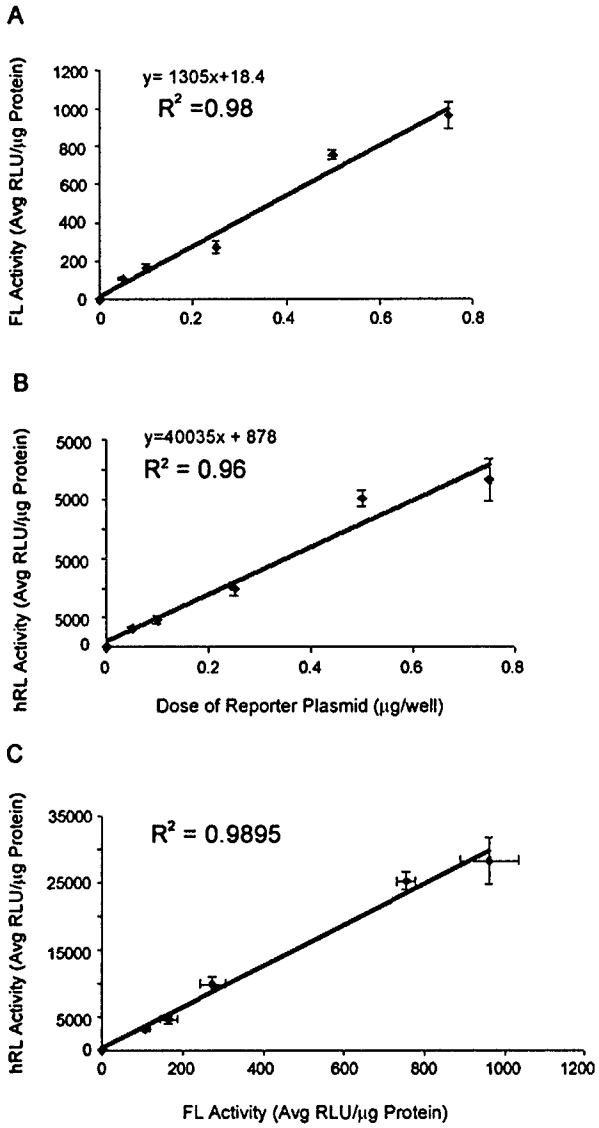

FIG. 4. Linear increase in gene expression with increasing levels of reporter plasmid. (**A**) and (**B**) show the linear relationship between the expression of *fl* (**A**) and *hrl* (**B**) genes and the dose of the reporter plasmid (*fl*-G5-*hrl*) (0–0.75 µg/well) while the dose of the activator plasmid was maintained at 0.5 µg/well. Seen here are high correlations (r^2 = 0.96 and 0.98 for *hrl* and *fl*, respectively) between the dose of reporter plasmid used for transfection and protein activities. The results were obtained 24 hr after transfection in N_{2a} cells. Error bars indicate the SEM for triplicate measurements. (**C**) Correlation between *hrl* and *fl* expression in N_{2a} cells transfected with various doses of *fl*-G5-*hrl* and a constant dose of VP16. The correlation is r^2 = 0.99.

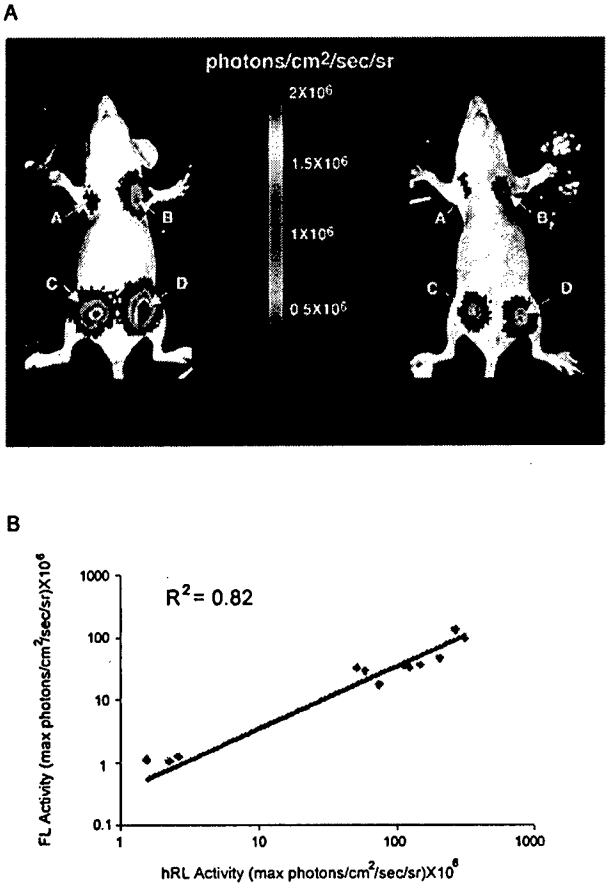

FIG. 5. (A) Optical CCD imaging of a mouse carrying N_{2a} cells transiently cotransfected with a constant dose of *fl*-G5-*hrl* and various doses of the activator plasmid VP16 implanted subcutaneously at four different sites. Sites A–D indicate cells transfected with various doses of VP16 in increasing order. Both images shown are from the same mouse and are formed by superimposing visible light images on the optical CCD bioluminescence image with a scale depicting photons/cm^2/sec/steradian (sr). Mice were imaged after tail vein injection of coelenterazine (*left*) and after intraperitoneal injection of D-luciferin (*right*). (**B**) Correlation of *fl* and *hrl* gene expression from three mice optically imaged with cells cotransfected with different doses of the activator plasmid (VP16) and a constant dose of the reporter plasmid (*fl*-G5-*hrl*). Shown is a plot of hRL activity versus FL activity, expressed as maximum photons/cm^2/sec/sr, obtained from ROIs drawn over the implantation sites on the mouse images ($r^2 = 0.82$, $n = 3$ mice).

in cells implanted and imaged in living animals. N_{2a} cells were cotransfected with various doses of the activator plasmid and a constant dose of the reporter plasmid in six-well plates. The dose of the reporter plasmid was maintained at 0.67 μg/well while the activator dose was varied (10, 50, 100, and 150% of the reporter [*fl*-G5-*hrl*] dose). Cells were harvested after 24 hr and 1×10^6 cells were implanted separately at four different sites in each of three male nude mice. The mice were then scanned with the cooled CCD camera to image the activities of the luciferases from each site. The mice were first scanned after tail vein injection of coelenterazine. Five hours later the mice were scanned again after an intraperitoneal injection of D-luciferin. There is a linear increase in the expression levels of both genes across mice for the dose range tested (Fig. 5A). Furthermore, the expression levels of both reporter genes, measured as ROI values (maximum photons/cm^2/sec/steradian) for each implantation site is well correlated ($r^2 = 0.82$) in living mice (Fig. 5B).

Next, we wanted to test the efficacy of this amplification system in a real gene therapy application. For this purpose we injected the components of this system in a 1:1 ratio (10 μg of each of the plasmids) by the method of hydrodynamic injection into the tail vein of living mice. Naked DNAs delivered by this process are delivered to the liver, where they tend

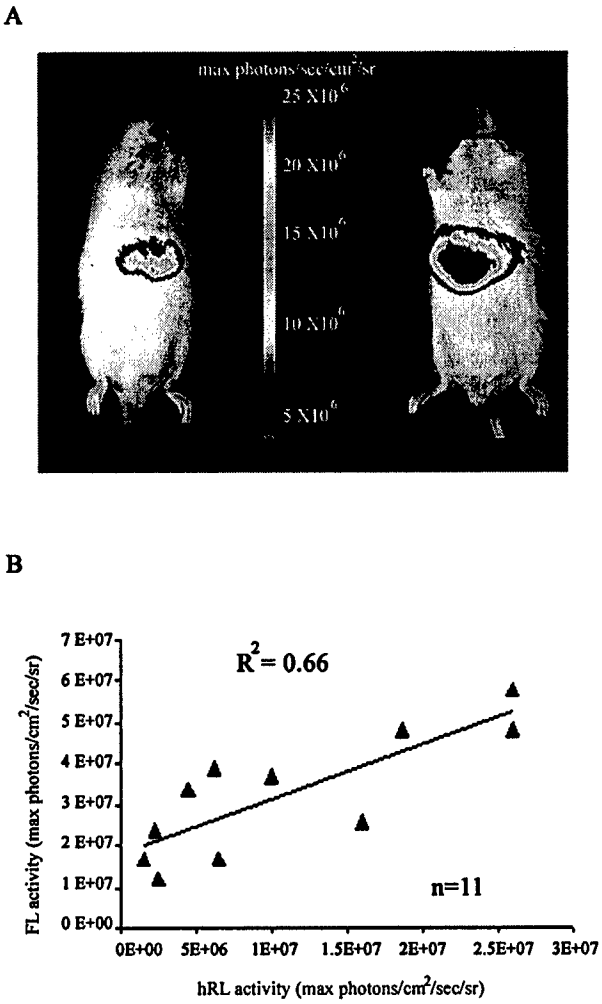

FIG. 6. (A) Optical CCD imaging of a mouse injected hydrodynamically with 10 μg each of activator (VP16) and reporter plasmid (*fl*-G5-*hrl*) 24 hr before imaging. Both images shown are from the same mouse and are formed by superimposing visible light images on the optical CCD bioluminescence image with a scale depicting photons/cm^2/sec/sr. Mice were imaged after tail vein injection of coelenterazine (40 μg; *left*) and after intraperitoneal injection of D-luciferin (3 mg; *right*). (**B**) Correlation of *fl* and *hrl* gene expression from mice optically imaged after the injection of 10 μg each of the activator plasmid (VP16) and the reporter plasmid (*fl*-G5-*hrl*). Shown is a plot of hRL activity versus FL activity, expressed as maximum photons/cm^2/sec/sr, obtained from same-sized ROIs drawn over the liver region on the mouse images ($r^2 = 0.66$, $n = 11$ mice).

to transfect the liver hepatocytes *in vivo* with high efficiency (Zhang *et al.*, 1999). We wanted to test whether our system would be able to produce detectable expression of the two reporter genes and also retain the high degree of correlation between the gene expression levels in the hepatocytes transfected *in vivo* by this technique. Indeed, we could detect robust expressions of both *fl* and *hrl* reporter genes in the liver regions of the animals within 6 hr of hydrodynamic injection and expression was still high even 24 hr after the injection (Fig. 6A). Most importantly, the level of expression of the *hrl* gene is also well correlated ($r^2 = 0.66$) with that of the *fl* gene in living mice ($n = 11$) (Fig. 6B).

DISCUSSION

This article reports initial results from experiments in which a novel GAL4-responsive bidirectional vector was used to amplify the expression of two reporter genes simultaneously both in cell culture and in living animals. This system should help to amplify the expression of a gene of interest from a weak tissue-specific promoter and to determine the spatial location and level of expression of the target gene repeatedly, with the help of the highly correlated expression of a tightly coupled reporter gene. This approach can be made fully quantitative and tomographic by simply replacing the optical reporter gene with a PET reporter gene.

We have previously demonstrated that the TSTA strategy can be used to amplify the expression of a single reporter gene from a weak tissue-specific promoter in a prostate-specific manner in living mice (Iyer *et al.*, 2001). We have been evaluating ways to develop this system as a potential gene therapy vector. Accordingly, we decided to design a bidirectional system based on the TSTA model that will link a therapeutic gene with an imaging reporter gene, so that, as stated previously, by simply studying the reporter gene noninvasively we can estimate the magnitude of expression of our target gene of interest and also monitor its location. Such a system may also be useful in transgenic animal applications, where the expression of the gene of interest can be repeatedly monitored in an intact animal.

In the present study we observed that expression from both coding regions was significantly elevated and retained a high level of correlation. Our data demonstrate that the hRL signal resulting from translation of the forward *hrl* gene in the bidirectional reporter vector can be used to quantify the level of expression of the *fl* gene in living animals. However, there was apparently a significant attenuation of the *fl* gene placed in a reverse orientation to the GAL4-binding sites in the vector. Despite this, we could observe robust signal from the *fl* gene both in cell culture and *in vivo*. Most importantly, we also obtained a high correlation between the expression levels of the two reporter genes both in cell culture ($r^2 = 0.95$) and in living animals ($r^2 = 0.82$ and 0.66), using bioluminescence imaging.

The naked DNA experiments were performed to test the efficacy of the system developed in a real gene therapy application, in which the different components of this system will be delivered *in vivo* by means of different nonviral or viral vectors and will be required to transfect the cells of the animal *in situ*. Earlier studies have shown that efficient plasmid delivery to the liver can be achieved via a hydrodynamically based procedure involving rapid tail vein injection of a large volume of DNA solution (Liu and Knapp, 2001; Herweijer and Wolff, 2003). This method is being widely utilized by gene therapy researchers to evaluate the therapeutic activities of various genes (Zhang *et al.*, 2004). We decided to adopt this method to transfect hepatocytes *in vivo* with both activator and reporter plasmids and then study whether the correlation was still maintained between the levels of expression of the two genes. We obtained a good level of correlation between the two reporter genes ($r^2 = 0.66$), similar to what was seen in the xenograft studies. These results support the robustness of our system. However, in contrast to the xenograft studies, in the naked DNA experiments we had to administer a higher dose of coelenterazine to obtain a detectable signal for the *hrl* reporter gene. This was expected because *Renilla* luciferase is known to produce blue-shifted light (475 nm) that is largely attenuated while traveling from a deep tissue environment like the liver. Apart from this there could be other parameters that regulate the delivery of the substrate coelenterazine to the transfected hepatocytes, such as the hepatic circulation and the presence of P-glycoproteins (Ros *et al.*, 2003; Pichler *et al.*, 2004). All these factors can also be influential in achieving a lower correlation compared with subcutaneous tumor studies, in which the source of light has a superficial location.

The bidirectional system showed a 3- to 4-fold lower expression of the *fl* gene when compared with a well-established reporter system, CMV-*fl*, and a 2- to 3-fold lower signal of the forward *hrl* gene when compared with CMV-*hrl*. An earlier TSTA system also showed a 2- to 3-fold lower signal from a SV40-GAL4-VP16-activated unidirectional G5-*fl* vector when compared with CMV-*fl* (Iyer *et al.*, 2001). Thus a reduced signal from the forward *hrl* gene when compared with CMV-*hrl* is in accordance with previous results. Previous studies have validated that 5×GAL4-binding sites are optimal for one promoter (Emami and Carey, 1992; Iyer *et al.*, 2001; Zhang *et al.*, 2002). Thus it could be possible that the inclusion of an additional promoter might compete with the available GAL4-VP16 activator proteins, thereby resulting in a reduction of overall activities of both promoters. However, we are unable to explain the phenomenon causing a greater attenuation of the expression level of the reverse gene. On the basis of other studies (Ross *et al.*, 2000; Dion and Coulombe, 2003) it seems unlikely that this effect is related to the orientation of the GAL4-DNA-binding domains. It has been observed that the ability of GAL4-VP16 to activate transcription varies 1- to 2-fold with 2- to 8-bp variations in the spatial positioning of the DNA-bound activation domain from the TATA box of the promoter (Ross *et al.*, 2000). Thus it is possible that slight dissimilarities in the spacer distances between the individual E4TATA minimal promoters and the GAL4-binding sites in the reporter plasmid can impart differential transcriptional abilities to the promoters, resulting in turn in differential expression of the genes they activate. Uneven spacer distances between the coding sequences of the two genes and their minimal promoters may also cause this effect. In our vector system the reverse *fl* gene is 30 bp away from its E4TATA minimal promoter, whereas the forward *hrl* gene is only 10 bp away. We are currently trying to test these possibilities by simply switching the positions of the two genes and repeating the experiments with the new reporter vector.

Nonetheless, our initial results indicate for the first time that the TSTA strategy can be developed into a potent bidirectional system that can successfully achieve amplification of two independent genes, simultaneously. There are several ways we can try to reduce the attenuation of the reverse gene and make the system more robust. These include (1) optimization of the number of GAL4-binding sites for two promoters, (2) optimization of the spacer distance between the genes and the minimal promoter, (3) optimization of the spacer distance between the minimal promoter and the GAL4-binding sites, and (4) use of a more potent transcriptional activator that contains two activator domains of VP16 fused to the GAL4-DNA-binding domain (GAL4-VP2) (Zhang *et al.*, 2002).

We have observed a linear increase in the levels of expression of both genes as we increased the dose of the activator. However, the relationship may not hold true at higher concentrations of the activator, as earlier studies have shown attenuation of gene expression in the presence of excess GAL4-VP16 ("squelching") (Gill and Ptashne, 1988). We also observed that the bidirectional vector is somewhat leaky before being activated by GAL4-VP16; however, this leakiness gave rise to minimal background levels in both cell and animal studies.

Because it is important that any reporter gene-imaging approach not significantly perturb the cell or the animal models being studied we decided to do a dose–response study with various doses of the activator plasmid in various mammalian cell lines. Among the mammalian cell lines tested only transiently transfected 293T cells showed some levels of cytotoxicity at the highest dose (0.75 μg/well) used. Such effects were not observable in N_{2a} or HeLa cells. But because low levels of GAL4-VP16 were practically nondeleterious to the cells and still produced significant amplification of gene expression, we think that this system will be satisfactorily nontoxic. However, further studies with stable cell lines, gene therapy vectors, and transgenic animal models will help in the characterization of the potential toxicities of the current approach.

The bidirectional reporter system has many advantages over other, alternative systems. A fusion protein approach has the disadvantage of not being generalizable, because for every new therapeutic gene the fusion approach would have to be validated. This approach has an advantage over the bicistronic IRES strategy because, unlike the IRES, this system is not likely to be affected by physiological stress (such as heat shock, hypoxia, and poisoning) that can confound the quantitation (Sun *et al.*, 2001). Approaches to deliver reporter and therapeutic genes via separate vectors require a higher viral dose leading to a potentially overwhelming immune response and possible disengagement of reporter gene and therapeutic gene expression at the single-cell level (Yaghoubi *et al.*, 2001).

The bidirectional vector system can be combined in a single-vector system and eventually used in a multitude of gene therapy studies. Apart from facilitating the repeated imaging of the location(s), magnitude, and time variation of the reporter gene expression, this system can also help in the quantification of therapeutic and "suicide" genes. The high correlation power of this model will help immensely in the application of reporter gene technology to animals and humans, thereby advancing research in multiple fields including the monitoring of human gene therapy (Yu *et al.*, 2000). A system like this will also be useful for studying tumor growth and regression after pharmacological intervention, studying protein–protein interactions (Paulmurugan *et al.*, 2002; Ray *et al.*, 2002; Paulmurugan and Gambhir, 2003), and developing model gene therapy vectors for monitoring site-specific delivery and expression of transgenes.

ACKNOWLEDGMENTS

We thank Xioaman Lewis (Crump Institute of Molecular Imaging, UCLA), Qian Wang (Stanford University), and Kim Le (Department of Biological Chemistry, UCLA) for assistance with this project. This work is supported in part by NIH grants R01 CA82214 and SAIRP R24 CA92865, Department of Energy contract DE-FC03-87ER60615, and CaP Cure.

REFERENCES

BARON, U., FREUNDLIEB, S., GOSSEN, M., and BUJARD, H. (1995). Co-regulation of two gene activities by tetracycline via a bidirectional promoter. Nucleic Acids Res. **23,** 3605–3606.

BHAUMIK, S., and GAMBHIR, S.S. (2002a). Optical imaging of *Renilla* luciferase reporter gene expression in living mice. Proc. Natl. Acad. Sci. U.S.A. **99,** 377–382.

BHAUMIK, S., and GAMBHIR, S.S. (2002b). Simultaneous imaging of the expression of two bioluminescent reporter genes in living mice. Mol. Ther. **5,** S422.

BLAKE, P., JOHNSON, B., and VANMETER, J.W. (2003). Positron emission tomography (PET) and single photon emission computed tomography (SPECT): Clinical applications. J. Neuroophthalmol. **23,** 34–41.

CHAPPELL, S.A., EDELMAN, G.M., and MAURO, V.P. (2000). A 9-nt segment of a cellular mRNA can function as an internal ribosome entry site (IRES) and when present in linked multiple copies greatly enhances IRES activity. Proc. Natl. Acad. Sci. U.S.A. **97,** 1536–1541.

CONTAG, C.H., and BACHMANN, M.H. (2002). Advances in *in vivo* bioluminescence imaging of gene expression. Annu. Rev. Biomed. Eng. **4,** 235–260.

CONTAG, C.H., and ROSS, B.D. (2002). It's not just about anatomy: *In vivo* bioluminescence imaging as an eyepiece into biology. J. Magn. Reson. Imaging **16,** 378–387.

DION, V., and COULOMBE, B. (2003). Interactions of a DNA-bound transcriptional activator with the TBP-TFIIA-TFIIB-promoter quaternary complex. J. Biol. Chem. **278,** 11495–11501.

ECKELMAN, W.C., TATUM, J.L., KURDZIEL, K.A., and CROFT, B.Y. (2000). Quantitative analysis of tumor biochemistry using PET and SPECT. Nucl. Med. Biol. **27,** 633–635.

EMAMI, K.H., and CAREY, M. (1992). A synergistic increase in potency of a multimerized VP16 transcriptional activation domain. EMBO J. **11,** 5005–5012.

GAMBHIR, S.S., BARRIO, J.R., WU, L., IYER, M., NAMAVARI, M., SATYAMURTHY, N., BAUER, E., PARRISH, C., MACLAREN, D.C., BORGHEI, A.R., GREEN, L.A., SHARFSTEIN, S., BERK, A.J., CHERRY, S.R., PHELPS, M.E., and HERSCHMAN, H.R. (1998). Imaging of adenoviral-directed herpes simplex virus type 1 thymidine kinase reporter gene expression in mice with radiolabeled ganciclovir. J. Nucl. Med. **39,** 2003–2011.

GAMBHIR, S.S., BAUER, E., BLACK, M.E., LIANG, Q., KOKORIS, M.S., BARRIO, J.R., IYER, M., NAMAVARI, M., PHELPS, M.E., and HERSCHMAN, H.R. (2000). A mutant herpes simplex virus type 1 thymidine kinase reporter gene shows improved sensitivity for imaging reporter gene expression with positron emission tomography. Proc. Natl. Acad. Sci. U.S.A. **97,** 2785–2790.

GILL, G., and PTASHNE, M. (1988). Negative effect of the transcriptional activator GAL4. Nature **334**, 721–724.

HERWEIJER, H., and WOLFF, J.A. (2003). Progress and prospects: naked DNA gene transfer and therapy. Gene Ther. **10**, 453–458.

IYER, M., WU, L., CAREY, M., WANG, Y., SMALLWOOD, A., and GAMBHIR, S.S. (2001). Two-step transcriptional amplification as a method for imaging reporter gene expression using weak promoters. Proc. Natl. Acad. Sci. U.S.A. **98**, 14595–14600.

LAMMERTSMA, A.A. (2001). PET/SPECT: Functional imaging beyond flow. Vision Res. **41**, 1277–1281.

LIU, D., and KNAPP, J.E. (2001). Hydrodynamics-based gene delivery. Curr. Opin. Mol. Ther. **3**, 192–197.

LUKER, G.D., and PIWNICA-WORMS, D. (2001). Molecular imaging *in vivo* with PET and SPECT. Acad. Radiol. **8**, 4–14.

MASSOUD, T.F., and GAMBHIR, S.S. (2003). Molecular imaging in living subjects: seeing fundamental biological processes in a new light. Genes Dev. **17**, 545–580.

NEGRIN, R.S., EDINGER, M., VERNERIS, M., CAO, Y.A., BACHMANN, M., and CONTAG, C.H. (2002). Visualization of tumor growth and response to NK-T cell based immunotherapy using bioluminescence. Ann. Hematol. **81**(Suppl. 2), S44–S45.

NETTELBECK, D.M., JEROME, V., and MULLER, R. (1998). A strategy for enhancing the transcriptional activity of weak cell type-specific promoters. Gene Ther. **5**, 1656–1664.

NETTELBECK, D.M., JEROME, V., and MULLER, R. (2000). Gene therapy: Designer promoters for tumour targeting. Trends Genet. **16**, 174–181.

PAULMURUGAN, R., and GAMBHIR, S.S. (2003). Monitoring protein–protein interactions using split synthetic *Renilla* luciferase protein-fragment-assisted complementation. Anal. Chem. **75**, 1584–1589.

PAULMURUGAN, R., UMEZAWA, Y., and GAMBHIR, S.S. (2002). Noninvasive imaging of protein–protein interactions in living subjects by using reporter protein complementation and reconstitution strategies. Proc. Natl. Acad. Sci. U.S.A. **99**, 15608–15613.

PICHLER, A., PRIOR, J.L., and PIWNICA-WORMS, D. (2004). Imaging reversal of multidrug resistance in living mice with bioluminescence: MDR1 P-glycoprotein transports coelenterazine. Proc. Natl. Acad. Sci. U.S.A. **101**, 1702–1707.

QIAO, J., DOUBROVIN, M., SAUTER, B.V., HUANG, Y., GUO, Z.S., BALATONI, J., AKHURST, T., BLASBERG, R.G., TJUVAJEV, J.G., CHEN, S.H., and WOO, S.L. (2002). Tumor-specific transcriptional targeting of suicide gene therapy. Gene Ther. **9**, 168–175.

RAY, P., BAUER, E., IYER, M., BARRIO, J.R., SATYAMURTHY, N., PHELPS, M.E., HERSCHMAN, H.R., and GAMBHIR, S.S. (2001). Monitoring gene therapy with reporter gene imaging. Semin. Nucl. Med. **31**, 312–320.

RAY, P., PIMENTA, H., PAULMURUGAN, R., BERGER, F., PHELPS, M.E., IYER, M., and GAMBHIR, S.S. (2002). Noninvasive quantitative imaging of protein–protein interactions in living subjects. Proc. Natl. Acad. Sci. U.S.A. **99**, 3105–3110.

RAY, P., WU, A.M., and GAMBHIR, S.S. (2003). Optical bioluminescence and positron emission tomography imaging of a novel fusion reporter gene in tumor xenografts of living mice. Cancer Res. **63**, 1160–1165.

ROS, J.E., LIBBRECHT, L., GEUKEN, M., JANSEN, P.L., and ROSKAMS, T.A. (2003). High expression of MDR1, MRP1, and MRP3 in the hepatic progenitor cell compartment and hepatocytes in severe human liver disease. J. Pathol. **200**, 553–560.

ROSS, E.D., KEATING, A.M., and MAHER, L.J., III. (2000). DNA constraints on transcription activation *in vitro*. J. Mol. Biol. **297**, 321–334.

SHARMA, V., LUKER, G.D., and PIWNICA-WORMS, D. (2002). Molecular imaging of gene expression and protein function *in vivo* with PET and SPECT. J. Magn. Reson. Imaging **16**, 336–351.

SUN, X., ANNALA, A.J., YAGHOUBI, S.S., BARRIO, J.R., NGUYEN, K.N., TOYOKUNI, T., SATYAMURTHY, N., NAMAVARI, M., PHELPS, M.E., HERSCHMAN, H.R., and GAMBHIR, S.S. (2001). Quantitative imaging of gene induction in living animals. Gene Ther. **8**, 1572–1579.

SUNDARESAN, G.G., and GAMBHIR, S.S. (2002). Radionuclide imaging of reporter gene expression. In *Brain Mapping: The Methods*, 2nd ed. A.W. Toga and J.C. Mazziotta, eds. (Academic Press, San Diego, CA) pp. 799–818.

WANG, Y.A.G.S. (2001). New approaches for linking PET and therapeutic reporter gene expression for imaging gene therapy with increased sensitivity. Presented at the Society for Nuclear Medicine Meeting, Toronto, ON, Canada.

WEBER, W.A., HAUBNER, R., VABULIENE, E., KUHNAST, B., WESTER, H.J., and SCHWAIGER, M. (2001). Tumor angiogenesis targeting using imaging agents. Q. J. Nucl. Med. **45**, 179–182.

YAGHOUBI, S.S., WU, L., LIANG, Q., TOYOKUNI, T., BARRIO, J.R., NAMAVARI, M., SATYAMURTHY, N., PHELPS, M.E., HERSCHMAN, H.R., and GAMBHIR, S.S. (2001). Direct correlation between positron emission tomographic images of two reporter genes delivered by two distinct adenoviral vectors. Gene Ther. **8**, 1072–1080.

YU, Y., ANNALA, A.J., BARRIO, J.R., TOYOKUNI, T., SATYAMURTHY, N., NAMAVARI, M., CHERRY, S.R., PHELPS, M.E., HERSCHMAN, H.R., and GAMBHIR, S.S. (2000). Quantification of target gene expression by imaging reporter gene expression in living animals. Nat. Med. **6**, 933–937.

ZHANG, G., GAO, X., SONG, Y.K., VOLLMER, R., STOLZ, D.B., GASIOROWSKI, J.Z., DEAN, D.A., and LIU, D. (2004). Hydroporation as the mechanism of hydrodynamic delivery. Gene Ther. **11**, 675–682.

ZHANG, L., ADAMS, J.Y., BILLICK, E., ILAGAN, R., IYER, M., LE, K., SMALLWOOD, A., GAMBHIR, S.S., CAREY, M., and WU, L. (2002). Molecular engineering of a two-step transcription amplification (TSTA) system for transgene delivery in prostate cancer. Mol. Ther. **5**, 223–232.

ZHANG, W., CONTAG, P.R., MADAN, A., STEVENSON, D.K., and CONTAG, C.H. (1999). Bioluminescence for biological sensing in living mammals. Adv. Exp. Med. Biol. **471**, 775–784.

Address reprint requests to:
Dr. Sanjiv S. Gambhir
Stanford University School of Medicine
James H. Clarke Center
318 Campus Drive, E 150
Stanford, CA 94305-5427

E-mail: sgambhir@stanford.edu

Received for publication September 10, 2003; accepted after revision May 13, 2004.

Published online: June 22, 2004.

Functionality of Androgen Receptor-based Gene Expression Imaging in Hormone Refractory Prostate Cancer

[1]Makoto Sato, [1,2]Mai Johnson, [3]Liqun Zhang, [4,5,6,7]Sanjiv S Gambhir, [3,5,6]Michael Carey, and [1,4,5,6]Lily Wu

[1]Department of Urology, [2]Molecular Cellular & Integrative Physiology, [3]Biological Chemistry, [4]Molecular and Medical Pharmacology; [5]Crump Institute for Molecular Imaging, and [6]Jonsson Comprehensive Cancer Center, David Geffen School of Medicine, University of California Los Angeles; and [7]Department of Radiology and the Bio-X Program, Stanford University

Research supports:
Department of Defense DAMD17-03-1-0095 to LW.
NIH R01 CA101904 to LW.
Department of Defense DAMD PC 020177 to MC.
NIH R01 CA82214 (to SSG), SAIRP R24 CA92865 (to SSG).
An interdisciplinary grant from Jonsson Comprehensive Cancer Center to MC, LW and SSG.
DOD CDMRP postdoctoral fellowship (PC020531) to MS.

Correspoding author:
Lily Wu, MD, PhD.
Tel: 310-794-4390
Fax: 310-825-3027
675 Charles Young Dr S, Los Angeles, CA 90095.

Running Title: AR-based Gene Expression Imaging in HRPC

Key Words: prostate cancer, AR, molecular imaging, prostate-specific promoter, gene therapy

ABSTRACT

Purpose: A highly augmented, prostate-specific two-step transcriptional amplification (TSTA) method was developed with the ultimate goal of delivering an effective and safe gene-based treatment to prostate cancer patients. Due to the fact that very limited treatment options are available for recurrent hormone refractory prostate cancer (HRPC), it is imperative to assess whether the prostate specific antigen (PSA) promoter-based TSTA gene therapy will be functional in HRPC. **Experimental Design**: We tested the TSTA-driven adenovirus vector on three androgen-dependent and six HRPC models. Real-time gene expression was monitored by both optical imaging and the combined modality of Positron Emission Tomography (PET) and computed tomography (CT). **Results**: The TSTA-driven firefly luciferase expressing adenoviral vector was active in all androgen receptor (AR) expressing HRPC models, but inactive in AR- and PSA-negative lines. Interestingly, the TSTA-mediated gene expression was induced by hydrocortisone in MDA PCa 2b, a cell line with mutated AR that possesses altered ligand specificity. In animal models, the TSTA-mediated optical signal was more robust in the HRPC than androgen-dependent tumors. In a parallel trend, a TSTA vector that expresses the herpes simplex virus thymidine kinase PET reporter gene also displayed more robust PET signal in the HRPC tumor. **Conclusions**: The activity of TSTA system is AR dependent, and it recapitulates the functional status of endogenous AR. These data support the conclusion that AR function is activated in HRPC despite castrated levels of androgen. Together with the fact that majority of recurrent prostate cancers express AR and PSA, we foresee the TSTA approach can be a promising gene therapy strategy for the advanced stages of prostate cancer.

INTRODUCTION

Although recent data suggest that the death rate from prostate cancer is decreasing by 4% per year since 1994, it is still the second leading cause of cancer death in men, with an estimated 230,110 new cases and 29,900 deaths in the US in 2004 (1). About one-third of men with prostate cancer believed to have localized disease will already have micro-metastasis at the time of therapy (2). Despite treatment with surgery, 20 to 30% of the patients will suffer from disease recurrence as defined by serum PSA elevation (3, 4). In the aggressive, high grade (Gleason 8-10) disease, majority of PSA recurrence is detected within 2 years after surgery with median survival of less than 3 years (3). Hormone therapy blocking androgen function can induce short-term remission, but the refractory disease eventually recurs (2). At this stage, the disease is defined as androgen-independent or hormone-refractory prostate cancer (HRPC). The median survival for patients with metastatic HRPC is about 18 months, and systemic chemotherapy provides only a palliation of symptoms (5).

Androgen receptor (AR), the mediator of the physiological effects of androgen (6), regulates the growth of normal and malignant prostate epithelial cells. Following the binding of the activating ligand dihydrotestosterone, AR translocates from the cytoplasm into the nucleus, binds directly to DNA recognition sites and induces the expression of androgen responsive genes, including PSA. A central issue in HRPC is to understand the role of AR in this stage of disease. Would AR function be obsolete under treatment where the activating ligand was depleted? Several mechanisms have indicated the continual involvement of AR in HRPC (reviewed in 7), including 1) AR gene amplification and overexpression; 2) altered ligand specificity of AR (promiscuous AR); and 3) activation of AR through cross-talks with other androgen-independent pathways. The precise role of AR in clinical situations is not fully understood. However, given the fact that AR expression is documented in the majority

of HRPC cases (8, 9) and that PSA remains the most reliable marker for recurrent, metastatic prostate cancer (10), it is highly probable the gene regulatory activity of AR is functional in this setting.

Several PSA or probasin promoter-based gene therapy approaches have been developed (11, reviewed in 12). However, thorough investigations questioning the functionality of these AR-dependent therapeutic strategies in HRPC have not been completed. The current report employs cell-based activity measurements and *in vivo* molecular imaging to demonstrate that a highly amplified PSA promoter-derived (TSTA) system is active in HRPC models. Non-invasive bioluminescence imaging and Positron Emission Tomography (PET) illustrate that the prostate-specific TSTA gene expression vectors exhibit robust activity in HRPC as well as androgen dependent tumors. We project that our vector-based gene therapy coupled to molecular imaging would be a promising therapeutic option to develop for treating patients with recurrent disease.

MATERIALS AND METHODS

Adenovirus Constructs.

AdTSTA-FL was constructed as previously described (13, 14). The AdTSTA-sr39tk was constructed with the AdEasy system (15). The head-to-head orientation of activator (BCVP2) and reporter (SR39tk) in the single plasmid was constructed by replacing FL with SR39tk in PBCVP2G5-L (16). The BCVP2G5-sr39tk fragment generated by *Not* I and *Sal* I digestion of PBCVP2G5-sr39tk was inserted into pShuttle, which was used in bacterial recombination to generate the full-length virus. The virus was grown on 293 cells, purified on a CsCl gradient, and titered by plaque formation assays on 293 monolayers. The level of replication competent adenovirus contamination in the viral stocks was evaluated by plaque formation on A549 cells. No plaque was detected at 10^8 fold higher viral stock dilution compared to assays on 293 cells.

Prostate Cell Lines and Luciferase Activity Assay.

The human prostate cancer cell lines, LNCaP, CWR22Rv1, DU145 and PC-3 were grown in RPMI 1640 supplemented with 10% fetal bovine serum (FBS). Iscove's modified DMEM was used for LAPC-4. MDA PCa 2b line obtained from ATCC was grown in BRFF-HPC1 (Athena Environmental Sciences, Baltimore, MD) supplemented with 20% FBS. For AdTSTA-FL assays, the cultured cells were plated onto 24-well plates at 5×10^4 cells per well with phenol-red free RPMI 1640 supplemented with 10% charcoal-stripped FBS. Cells were counted and infected at 1 plaque forming unit per cell (MOI=1). At 48 h post-infection, the cells were harvested and lysed in RIPA buffer (1% NP-40, 0.1% sodium deoxycholate, 150 mM NaCl, 50 mM Tris-HCl (pH7.5) and 1 mM PMSF). Luciferase activity was measured according to the manufacturer's instructions (Promega, Madison, WI), using a luminometer

(Berthold Detection Systems, Pforzheim, Germany). Each value was normalized with protein concentration and calculated as the average of triplicate samples. The infectivity of all cell lines was assessed by quantitative PCR of internalized viral DNA and expression mediated by constitutive AdCMV-FL as previously described (14). Relative to the infectivity of LNCaP cells (designated as 1), the infectivity of all other lines are within 2-fold. The highest infectivity was in CWR22rv1 (2.0) and the lowest was in PC-3 (0.7). Due to the similarity of infectivity among the cell lines, activity results reported here were not adjusted.

Synthetic androgen methylenetrienolone (R1881; NEN Life Science Products, Boston, MA) or the anti-androgen bicalutamide (Casodex) was added to experiments as indicated. To measure the androgen induction effect, we used the activity in the presence of 10 μM bicalutamide as the basal level rather than in charcoal-stripped FBS. The TSTA system is highly amplified and low level of residual androgen in charcoal-stripped FBS can activate expression (16). For western analysis, cell lysates were fractionated on 4-20% gradient acrylamide gels (BioRad, Hercules, CA) and subjected to immunoblot analysis with anti-AR N-20 (Santa Cruz, Santa Cruz, CA) or ß-actin A5316 (Sigma, St Louis, MO) antibodies, and visualized with HRP-labeled secondary antibody and ECL (Amersham, Piscataway, NJ).

Statistical analyses were performed using the two-tailed Student's t test. For all analyses, $P<0.01$ was considered statistically significant.

Preparation of tumor cell suspension.

Preparation of tumor cell suspensions was performed by slight modification of a published protocol (17). Briefly, tumors were harvested, minced to 1-mm^3, and then incubated in 1% Pronase (Roche Molecular Biochemicals, Mannheim, Germany) solution for 20 min at room temperature. After overnight incubation in PrEGM media (Cambrex,

Walkersville, MD) with Fungizone, the cultured cells were disaggregated by pipetting through sterile 200 μm Cell-Sieve mesh (Biodesign, Inc. of New York, Carmel, NY). Tumor cells were infected at 1 plaque forming unit per viable cell (MOI=1), and analyzed after 48 hrs. No difference in the infectivity (determined by infection with a green fluorescent protein expressing adenoviral vector) or non-specific viral toxicity was observed between the androgen-dependent and androgen-independent LAPC-9 tumor cells.

TK enzyme assay.

LNCaP and LAPC-4 were plated onto 6-well plates at 5 x 10^5 cells/well and infected with AdTSTA-sr39tk at MOI=1. 10 nM R1881 or 10 μM Casodex was added to the infected cells as indicated and the cells were harvested and lysed, in 0.5% NP-40, 25mM NaF, 3 mM ß-mercaptoethanol and 10 mM Tris-HCl (pH7.0) after 48 hr. The protein concentration of the cell lysates was determined by the DC protein assay (BioRad), 1 μg of the lysate was mixed with 3 μl of Tk mix ([^{3}H]-penciclovir (Movarek Biochemicals, Brea, CA), 250 mM Na_2HPO_4 (pH6.0), 25 mM ATP, 25 mM Mg Acetate) and incubated at 37°C for 20 min. Reactions were terminated by the addition of 40 μl cold water and heating at 95°C for 2 min. Forty μl of mixture was blotted onto DE81 filters (Whatman, Clifton, NJ). The filters were dried, and washed 3 times with 4 mM Ammonium formate and 10 μM thymidine, once in water, and twice in 95% ethanol. After drying, the filters were counted by scintillation. Each value was calculated as the average of duplicate samples.

Animal experiments with optical and PET imaging.

Animal care and procedures were performed in accordance with the University of California Animal Research Committee guidelines. Ten- to 12-week-old male SCID mice

obtained from Taconic Farms (Germantown, NY) were implanted subcutaneously with a tumor chunk (~0.2 cm dia) coated with Matrigel (Collaborative Research, Bedford, MA) and allowed to grow to ~0.8 cm dia (18). For the optical imaging experiments, 10^7 plaque-forming units of AdTSTA-FL were subdivided and injected intratumorally into 3 sites. *In vivo* expression was monitored sequentially using a cooled IVIS CCD camera (Xenogen, Alameda, CA). For each imaging session, the mice were anesthetized with ketamine/xylazine (4:1), given the D-luciferin substrate (200 µl of 150 mg/kg in PBS) intraperitoneally, and imaged after a 20-minute incubation. Images were analyzed with IGOR-PRO Living Image Software, as described (13, 19). Immunohistochemistry to detect AR expression in the tumor was performed with anti-AR antibody (Upstate Co, Charlottesville, VA) as previously described (13, 19).

For microPET imaging, 10^9 plaque-forming units (~30 µl) of AdTSTA-sr39tk were injected intratumorally for four consecutive days. PET imaging was performed on day 7 using ~200 µCi of [^{18}F]-FHBG substrate (specific activity 5-10 Ci/mmol) that was administered via the tail vein. After one hour of uptake time, mice were given inhalation isoflurane anesthesia, placed in a prone position, and imaged for 20 minutes in the microPET scanner (Concorde Microsystems, Knoxville, TN). Images were reconstructed using a filtered back projection reconstruction algorithm. MicroCT (Imtek Inc., Knoxville, TN) was performed for the same animal sequentially, and images were overlapped using ASIPro VM (Concorde Microsystems, Knoxville, TN).

RESULTS

The TSTA activity in prostate cancer cell lines

We have developed several transcriptionally-targeted gene expression systems based on the PSA gene regulatory regions. The method that exhibits most potent activity, tissue selectivity and androgen regulation is termed two-step transcriptional activation (TSTA). It employs an enhanced PSA promoter (20) that drives a potent GAL4VP16 synthetic activator, which in turn binds to tandem repeats of GAL4 binding sites to activate the secondary reporter or therapeutic gene. This TSTA method achieved nearly 1000-fold augmentation of activity over the native PSA promoter, and it is more active than the strong viral CMV promoter (14). Recently, we have demonstrated that AR in hormone refractory LAPC-9 tumors is functionally active, and it binds to known sites in the PSA gene regulatory region by chromatin immunoprecipitation (13). Expanding upon this observation, the key objective of this study is to survey the activity of TSTA vectors in a wider array of HRPC models and to visualize the *in vivo* activity of the vectors by multi-modal molecular imaging techniques.

The activity of the TSTA adenoviral vector (AdTSTA-FL, Figure 1A) was first determined in two AD lines LNCaP and LAPC-4, and three HRPC lines CWR22Rv1, DU145 and PC-3. As shown in Figure 1B, in the AR-negative DU145 and PC-3 lines AdTSTA-FL activity was negligible. In the three AR-expressing lines, the activity of AdTSTA-FL was stimulated by androgen ranging from 11.4- to 60.6-fold. When bicalutamide (10 μM) was given simultaneously in the presence of synthetic androgen R1881 (10 nM), a ~50% suppression of peak activity was observed (data not shown). In the presence of androgen, LNCaP cells exhibited the highest expression, at 4.8 times the level of LAPC-4 and 14.4 fold-higher than CWR22Rv1.

We also investigated the activation in a fourth HRPC line MDA PCa 2b, which interestingly, expresses AR with a double mutation (L701H and T877A) that allows gene expression and growth to become glucocorticoid responsive (21). As shown in Figure 1C, gene expression mediated by this promiscuous AR responded to both androgen and hydrocortisone. The induction was 105-fold by hydrocortisone and 144-fold by R1881. The absolute expression level in MDA PCa 2b was 4.4 fold-lower than CWR22Rv1. Based on these expression data, we deduced that the PSA-based TSTA method is active in HRPC but its activity is dictated by the AR function in the cell.

TSTA activity in hormone refractory LAPC-9 tumor monitored by optical imaging.

LAPC-9 and LAPC-4 are two human prostate tumors that can recapitulate the clinical scenario of HRPC (17, 18). They grow routinely in intact male mice and undergo tumor regression upon castration. However, after a substantial time-delay, hormone refractory tumor develops, mimicking the recurrence of HRPC. The activity of AdTSTA-FL was monitored by optical imaging of paired AD and hormone refractory LAPC-9 tumors from day 4 to 14 (Figure 2A). By this real-time *in vivo* activity measurement, hormone refractory tumors supported a higher level of transgene expression than AD tumors. Immunohistochemistry analysis revealed that the AR protein was expressed in both AD and HRPC tumors, but the magnitude of expression is very heterogenous among the tumor cells (Figure 2B).

Equivalent gene delivery into the different tumors by intratumoral viral injection was difficult to achieve. Thus, we converted the paired tumors into single cell suspension to examine androgen regulation and the activity of the TSTA system more accurately. In doing so, the dosage of viral vector and androgen administered on a per cell basis can be controlled. The dispersed tumor cells were infected with AdTSTA-FL in the presence of specified ligands.

AR-protein and androgen-responsive FL activity was observed in both cell populations (Figure 2C). In close agreement with the optical imaging results in tumors, we also observed that the activity of AdTSTA-FL is 7.2-fold higher in the hormone refractory (AI) than in AD tumor cells in culture in the presence of 1 nM or higher concentrations of R1881.

Use of the TSTA vector in PET imaging.

It is important to develop molecular imaging approaches that can be applied in clinical settings for advanced prostate cancer. To this end, we adapted our prostate-specific gene imaging to PET, a radionuclide functional imaging modality that enables 3-D signal localization. An adenoviral vector that expresses the herpes simplex virus thymidine kinase (HSV-tk) PET reporter gene under the control of TSTA was generated (Figure 3A). An enhanced HSV-tk variant sr39tk was incorporated into the AdTSTA-sr39tk because this variant tk gene augments the uptake of radiolabeled PET tracers and improves PET imaging sensitivity by 2-fold (22). The sr39tk protein expression and enzymatic activity mediated by the vector was regulated by androgen (Figure 3B, C).

AdTSTA-sr39tk was administered into AD and hormone refractory LAPC-4 tumors, and its activity was documented by the combined microPET/microCT. This combined imaging modality enables the precise localization of the PET signals with the anatomic information obtained from the CT scan. Using [^{18}F]-FHBG as the PET substrate, robust signals were observed in both AD and hormone refractory LAPC-4 tumors (Figure 3D). The activity was higher in the hormone refractory tumor (0.78% ID/g) than in the AD tumor (0.50% ID/g). These results confirm that the TSTA-mediated prostate-specific gene imaging is feasible for advanced stages of tumor using the clinically relevant PET.

DISCUSSION

Effective treatment options for recurrent prostate cancer are notably limited. Our goal has been to develop novel gene-based diagnostic and therapeutic approaches to treat advanced stages of prostate cancer. Towards this end, the well-studied PSA promoter/enhancer was utilized to achieve prostate-specific gene expression. Given that transcriptional regulation of the PSA promoter/enhancer is AR-dependent, it was prudent to first verify that our PSA promoter-based expression strategy is feasible in HRPC. In this study, we demonstrated that the highly amplified prostate-specific TSTA gene delivery vectors are indeed functional in many models of HRPC under androgen-deprived conditions.

Our data support that the presence of functional AR is necessary to activate PSA-based promoter constructs. However, other factor(s) are likely to modulate AR activity in HRPC cells. The 14-fold range of luciferase activity observed in different models does not correlate with the level of AR expression or the status of AR mutation in the cell lines. The AR in LAPC-4 is wild-type, while it contains the T877A mutation in LNCaP and the H874Y mutation in the ligand-binding domain of CWR22Rv1. Differential activity of co-activators of the AR pathway could modulate AR function *in vivo*. Gregory et al (23) reported elevated level of nuclear receptor coactivators, SRC1 and SRC2 in recurrent prostate cancer. Recently, Dr. Tindall's group also demonstrated that coactivator p300 confers increased growth and progression potential in prostate cancer (24). Many other growth signal pathways such as IGF, Her2 or IL6 can also modulate AR-mediated expression (reviewed in 7). Further investigations are needed to determine the precise AR activation mechanism in different case of HRPC.

Both optical imaging and PET illustrated higher TSTA activity in the hormone refractory xenograft subline versus the parental AD tumor in two models. These findings

endorse the idea that activation of AR function occurs despite the castrated level of androgen *in vivo*. A recent report by Chen et al. (25) showed that 3 to 5-fold elevated expression of AR is a cardinal distinguishing feature between paired AD and hormone refractory tumors. Their work also, supports that AR over-expression can lead to HRPC. In fact, the two models reported here were assessed in the gene expression profiling study (25). Moreover, our results demonstrated that the real-time assessment of AR functional activity in prostate tumors, including HRPC, can be accomplished by introducing TSTA Ads into the tumor.

In contemplating future applications in clinical settings, we postulate that the TSTA gene-expression strategy will be active in all PSA-positive prostate cancers, which include the recurrent metastatic disease. Previous histological evaluation of clinical materials have detected AR and PSA expression in all stages of prostate cancer (8, 26, 27). Recent preliminary results (reported at SPORE meeting July 2004, Baltimore MD) indicated that AR expression is detected in metastatic lesions, albeit at heterogeneous level. A subtype of HRPC, the neuroendocrine (NE) prostate cancer, lacks AR, and it is associated with poor prognosis (28, 29). We anticipate any AR-dependent gene expression approach will be inactive in NE tumor cells. However, solitary NE tumors are rare, as most NE tumor cells exist in small foci interspersed within conventional AR- and PSA-positive prostate adenocarcinoma. If an AR-dependent toxic gene therapy was apply to a mixed lesion, then indirect tumoricidal effects can be transmitted to NE tumor cells via conventional prostate cancer cells by bystander effects (12).

Linking molecular imaging to gene therapy is a favorable method to assess the performance of the intended treatment. In an earlier study, visualization of distant metastases of prostate tumor was accomplished by optical imaging mediated through the use of a modified PSA promoter-based adenoviral vector (19). Due to the inability of light energy to

penetrate deep into tissues, bioluminescence imaging is not applicable in humans. Thus, to translate the above-mentioned promising findings to the clinics, the application of a high-energy clinically-relevant modality such as PET is needed. However, the HSV-tk-based PET imaging is several orders of magnitude less sensitive than optical imaging in small animal studies (30). The nearly three-order gain in activity of TSTA over native PSA promoter is a key factor to achieve the successful PET imaging of HRPC. Since the same principles are at work in animal microPET as in clinical PET, this result supports the idea of an equivalent gene-based approach in clinical studies.

Many studies have demonstrated that the sr39tk gene can function effectively both as a PET reporter gene as well as a toxic suicide gene (12, 31). Recently, the AdTSTA-sr39tk was applied in a "one-two punch" imaging and suicide gene therapy to treat prostate tumor [Johnson et al. manuscript submitted]. Compared to a constitutive CMV-driven vector, the prostate-targeted TSTA vector not only elicited equivalent tumoricidal effects but also dramatically reduced systemic liver toxicity. The PET imaging correlated entirely with the therapeutic outcomes. These results indicate that the TSTA methodology is a promising platform to build gene-based diagnostic and therapeutic approaches to manage HRPC.

ACKNOWLEDGEMENT

We deeply appreciate the help of W. Ladno, J. Edwards, Dr. D. Stout for their skillful assistance in PET/CT imaging, Baohui Zhang for technical assistance, and the assistance of Giri Sulur on manuscript preparation. The CWR22Rv1 cell line and the polyclonal anti-tk antibody were kindly provided by Dr. David Agus and Dr. Margaret Black, respectively.

Figure legends

Figure 1. The activity of AdTSTA-FL and the induction with androgen in a panel of prostate cancer cell lines. A. Schematic representation of the AdTSTA-FL. The two TSTA components of activator (GAL4-VP16 driven by PSE-BC) and reporter (FL driven by 5xGAL4) are inserted into E1 region of recombinant adenovirus. B. AdTSTA-FL activity on a panel of prostate cancer cell lines. The cell lysates were harvested 2 days after infection and subjected to FL activity and western analysis with anti-AR antibody. Fold inductions calculated by the activity ratio with 10 nM R1881 over 10 μM casodex are indicated at the top in parentheses. The activity difference between the AR-positive cell lines and the AR-negative lines (DU-145 and PC-3) is statistically significant ($P<0.01$). C. AdTSTA-FL activity in MDA PCa 2b. The cells were infected and incubated with 10μM Casodex, 10nM R1881, and 5 and 50 nM hydrocortisone.

Figure 2. AdTSTA-FL-mediated activity *in vivo*. A. AdTSTA-FL-mediated optical signal in LAPC-9 AD and AI (androgen independent; HRPC) tumors. Ten million infectious units of virus were injected intratumorally and imaged by optical CCD camera on the specified day post viral injection. Common logarithms of the percentages of the signal at day 4 of AD and AI tumors are plotted in the right panel. B. AR protein in LAPC-9 tumors. Parafin-fixed thin tumor sections were stained with anti-AR antibody. C. AdTSTA-FL activity in tumor cell suspension prepared from LAPC-9 AD and AI (HRPC) tumors. Tumor cell suspension was infected with AdTSTA-FL at MOI=1 and incubated in the presence of 10μM Casodex or 0.1 or 10 nM R1881. The cell lysates were prepared after 2 days and subjected to FL assay and AR western blot. (C; 10 μM Casodex, R; 10 nM R1881). The activity difference between AI and AD cells in the presence of R1881 was statistically significant ($P<0.01$).

Figure 3. The activity of AdTSTA-sr39tk and its application in microPET. A. Schematic representation of the AdTSTA-sr39tk. The sr39tk gene is a HSV-tk variant with higher affinity for acycloguanosines. B. AdTSTA-sr39tk activity in AD prostate cancer cell lines LNCaP and LAPC-4. The cells were infected with AdTSTA-sr39tk at MOI=1 and harvested 2 days later. The cell lysates were subjected to TK enzyme assay. Phosphorylated forms of [^{3}H]-penciclovir were counted and plotted after normalization with total cellular protein. C. Androgen regulation of expression from AdTSTA-sr39tk. LNCaP cells were infected with AdTSTA-sr39tk at MOI=5 and incubated with 0 to 100 nM R1881. Cells were lysed and subjected to western analysis using anti-HSV-TK polyclonal antibody. D. Combined microPET and microCT of LAPC-4 AD and AI tumor. 4 x 10^{9} infectious units of AdTSTA-sr39tk was injected to AD and AI LAPC-4 tumors. One week later, [^{18}F]-FHBG injected animals were anesthetized and scanned for microPET and microCT sequentially. The signal in the tumor was measured by % injected dose of substrate per gram of tissue (%ID/g), listed below the image.

REFERENCES

1. Weir HK, Thun MJ, Hankey BF, Ries LA, Howe HL, Wingo PA, Jemal A, Ward E, Anderson RN, Edwards BK. Annual report to the nation on the status of cancer, 1975-2000, featuring the uses of surveillance data for cancer prevention and control. J Natl Cancer Inst 2003;95:1276-99.
2. Dowling AJ, Tannock IF. Systemic treatment for prostate cancer. Cancer Treat Rev 1998;24:283-301.
3. Pound CR, Partin AW, Eisenberger MA, Chan DW, Pearson JD, Walsh PC. Natural history of progression after PSA elevation following radical prostatectomy. JAMA 1999;281:1591-7.
4. Roehl KA, Han M, Ramos CG, Antenor JA, Catalona WJ. Cancer progression and survival rates following anatomical radical retropubic prostatectomy in 3,478 consecutive patients: long-term results. J Urol 2004;172:910-14.
5. Tannock IF, de Wit R, Berry WR, Horti J, Pluzanska A, Chi KN, Oudard S, Theodore C, James ND, Turesson I, Rosenthal MA, Eisenberger MA; TAX 327 Investigators. Docetaxel plus prednisone or mitoxantrone plus prednisone for advanced prostate cancer. N Engl J Med 2004;351:1502-12.
6. Gelmann EP. Molecular biology of the androgen receptor. J Clin Oncol 2002;20:3001-15.
7. Feldman BJ and Feldman D. The development of androgen-independent prostate cancer. Nat Rev Cancer 2001;1:34-45.
8. Hobisch A, Culig Z, Radmayr C, et al. Distant metastases from prostatic carcinoma express androgen receptor protein. Cancer Res 1995;55:3068-72.
9. Magi-Galluzzi C, Xu X, Hlatky L, et al. Heterogeneity of androgen receptor content in advanced prostate cancer. Mod Pathol 1997;10:839-45.
10. Bok RA and Small EJ. Bloodborne biomolecular markers in prostate cancer development and progression. Nat Rev Cancer 2002;2:918-26.
11. DeWeese TL, van der Poel H, Li S, et al. A phase I trial of CV706, a replication-competent, PSA selective oncolytic adenovirus, for the treatment of locally recurrent prostate cancer following radiation therapy. Cancer Res 2001;61:7464-72.
12. Wu L and Sato M. Integrated, molecular engineering approaches to develop prostate cancer gene therapy. Curr Gene Ther 2003;3:452-67.
13. Zhang L, Johnson M, Le KH, et al. Interrogating androgen receptor function in recurrent prostate cancer. Cancer Res 2003;63:4552-60.
14. Sato M, Johnson M, Zhang L, et al. Optimization of adenoviral vectors to direct highly amplified prostate-specific expression for imaging and gene therapy. Mol Ther 2003;8:726-37.
15. He TC, Zhou S, da Costa LT, et al. A simplified system for generating recombinant adenoviruses. Proc Natl Acad Sci U S A 1998;95:2509-14.
16. Zhang L, Adams JY, Billick E, et al. Molecular engineering of a two-step transcription amplification (TSTA) system for transgene delivery in prostate cancer. Mol Ther 2002;5:223-32.
17. Craft N, Chhor C, Tran C, et al. Evidence for clonal outgrowth of androgen-independent prostate cancer cells from androgen-dependent tumors through a two-step process. Cancer Res 1999;59:5030-6.

18. Klein KA, Reiter RE, Redula J, et al. Progression of metastatic human prostate cancer to androgen independence in immunodeficient SCID mice. Nat Med 1997;3:402-8.
19. Adams JY, Johnson M, Sato M, et al. Visualization of advanced human prostate cancer lesions in living mice by a targeted gene transfer vector and optical imaging. Nat Med 2002;8:891-7.
20. Wu L, Matherly J, Smallwood A, et al. Chimeric PSA enhancers exhibit augmented activity in prostate cancer gene therapy vectors. Gene Ther 2001;8:1416-26.
21. Zhao XY, Malloy PJ, Krishnan AV, et al. Glucocorticoids can promote androgen-independent growth of prostate cancer cells through a mutated androgen receptor. Nat Med 2000;6:703-6.
22. Gambhir SS, Bauer E, Black ME, et al. A mutant herpes simplex virus type 1 thymidine kinase reporter gene shows improved sensitivity for imaging reporter gene expression with positron emission tomography. Proc Natl Acad Sci U S A 2000;97:2785-90.
23. Gregory CW, He B, Johnson RT, et al. A mechanism for androgen receptor-mediated prostate cancer recurrence after androgen deprivation therapy. Cancer Res 2001;61:4315-9.
24. Debes JD, Sebo TJ, Lohse CM, et al. p300 in prostate cancer proliferation and progression. Cancer Res 2003;63:7638-40.
25. Chen CD, Welsbie DS, Tran C, et al. Molecular determinants of resistance to antiandrogen therapy. Nat Med 2004;10:33-9.
26. Sweat SD, Pacelli A, Bergstralh EJ, Slezak JM, and Bostwick DG. Androgen receptor expression in prostatic intraepithelial neoplasia and cancer. J Urol 1999;161:1229-32.
27. Koivisto PA and Helin HJ. Androgen receptor gene amplification increases tissue PSA protein expression in hormone-refractory prostate carcinoma. J Pathol 1999;189:219-23.
28. Krijnen JL, Bogdanowicz JF, Seldenrijk CA, et al. The prognostic value of neuroendocrine differentiation in adenocarcinoma of the prostate in relation to progression of disease after endocrine therapy. J Urol 1997;158:171-4.
29. di Sant'Agnese PA. Neuroendocrine differentiation in prostatic carcinoma: an update on recent developments. Ann Oncol 2001;12 Suppl 2:S135-40.
30. Ray P, Wu AM, and Gambhir SS. Optical bioluminescence and positron emission tomography imaging of a novel fusion reporter gene in tumor xenografts of living mice. Cancer Res 2003;63:1160-5.
31. Pantuck AJ, Matherly J, Zisman A, et al. Optimizing prostate cancer suicide gene therapy using herpes simplex virus thymidine kinase active site variants. Hum Gene Ther 2002;13:777-89.

Figure 1

A.

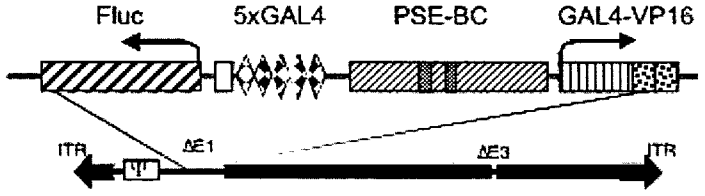
Fluc
5xGAL4
PSE-BC
GAL4-VP16
ITR
ΔE1
ΔE3
ITR

B.

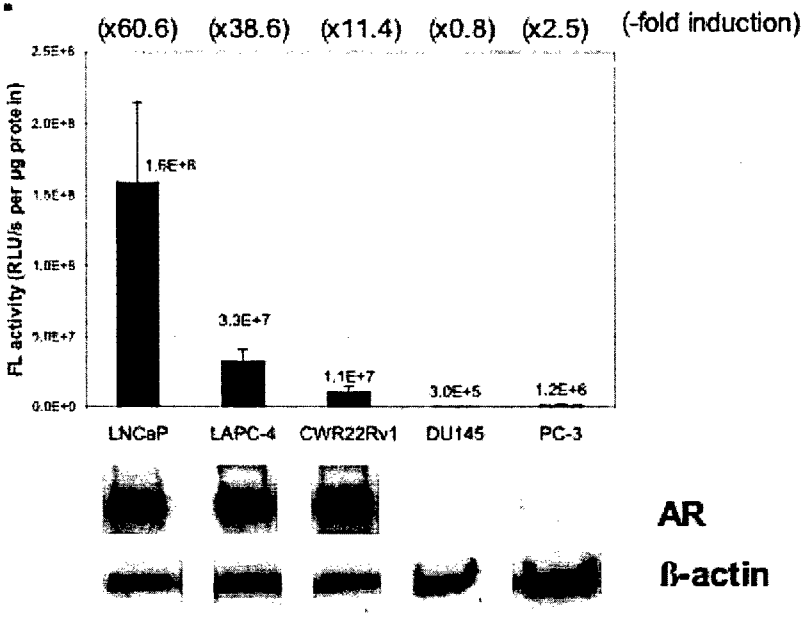
(x60.6)
(x38.6)
(x11.4)
(x0.8)
(x2.5)
(-fold induction)
FL activity (RLU/s per µg protein)
1.6E+8
3.3E+7
1.1E+7
3.0E+5
1.2E+6
LNCaP
LAPC-4
CWR22Rv1
DU145
PC-3
AR
ß-actin

C.

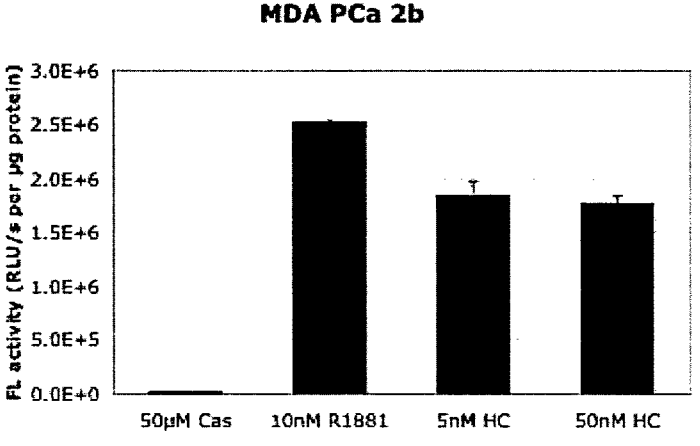
MDA PCa 2b
FL activity (RLU/s per µg protein)
3.0E+6
2.5E+6
2.0E+6
1.5E+6
1.0E+6
5.0E+5
0.0E+0
50µM Cas
10nM R1881
5nM HC
50nM HC

Figure 2

A.

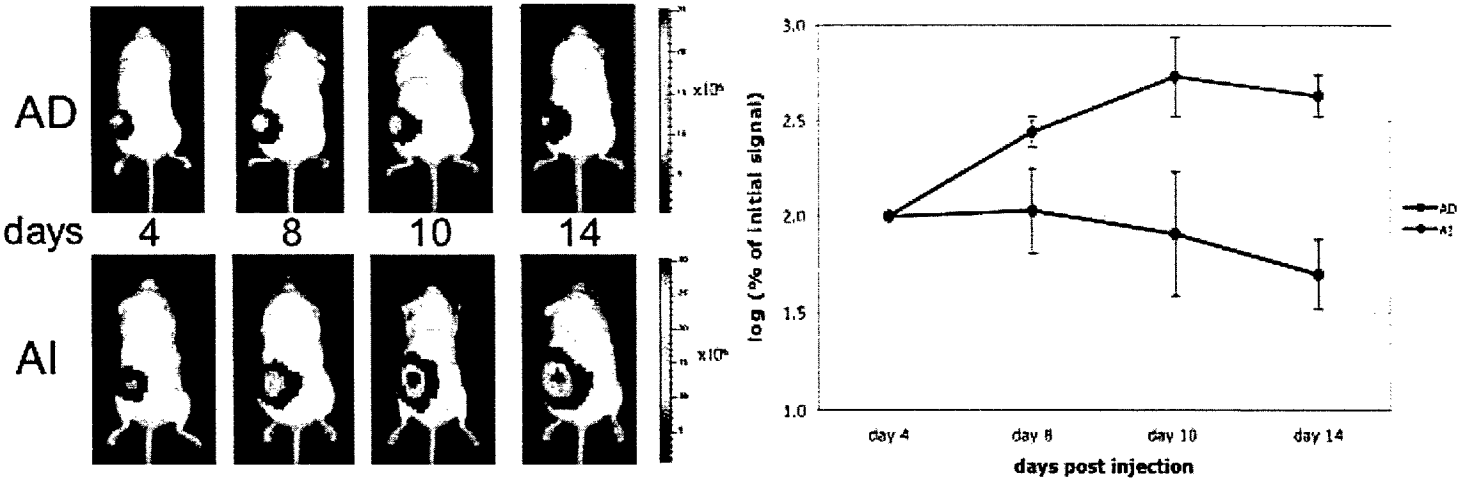
AD
days
4
8
10
14
AI
log (% of initial signal)
3.0
2.5
2.0
1.5
1.0
day 4
day 8
day 10
day 14
days post injection

B.

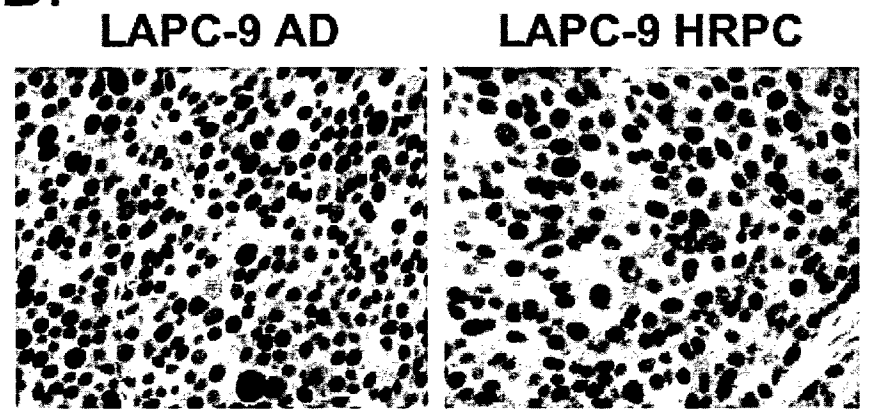
LAPC-9 AD
LAPC-9 HRPC

C.

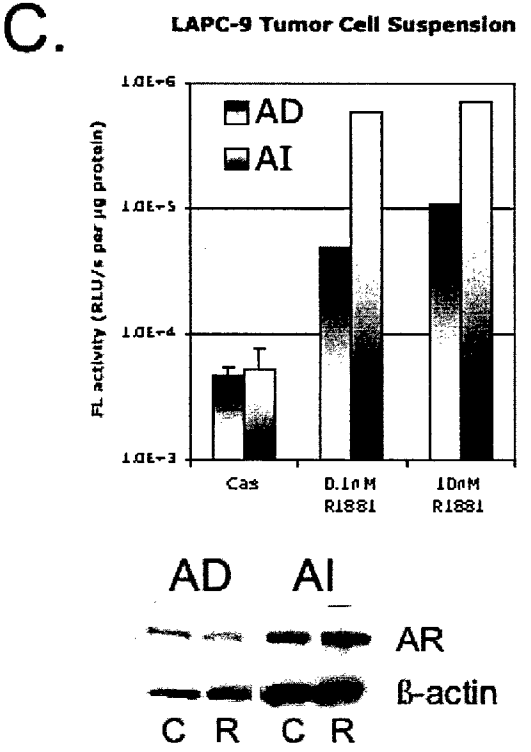
LAPC-9 Tumor Cell Suspension
AD
AI
FL activity (RLU/s per µg protein)
Cas
0.1nM R1881
10nM R1881
AD
AI
AR
ß-actin
C
R
C
R

Figure 3

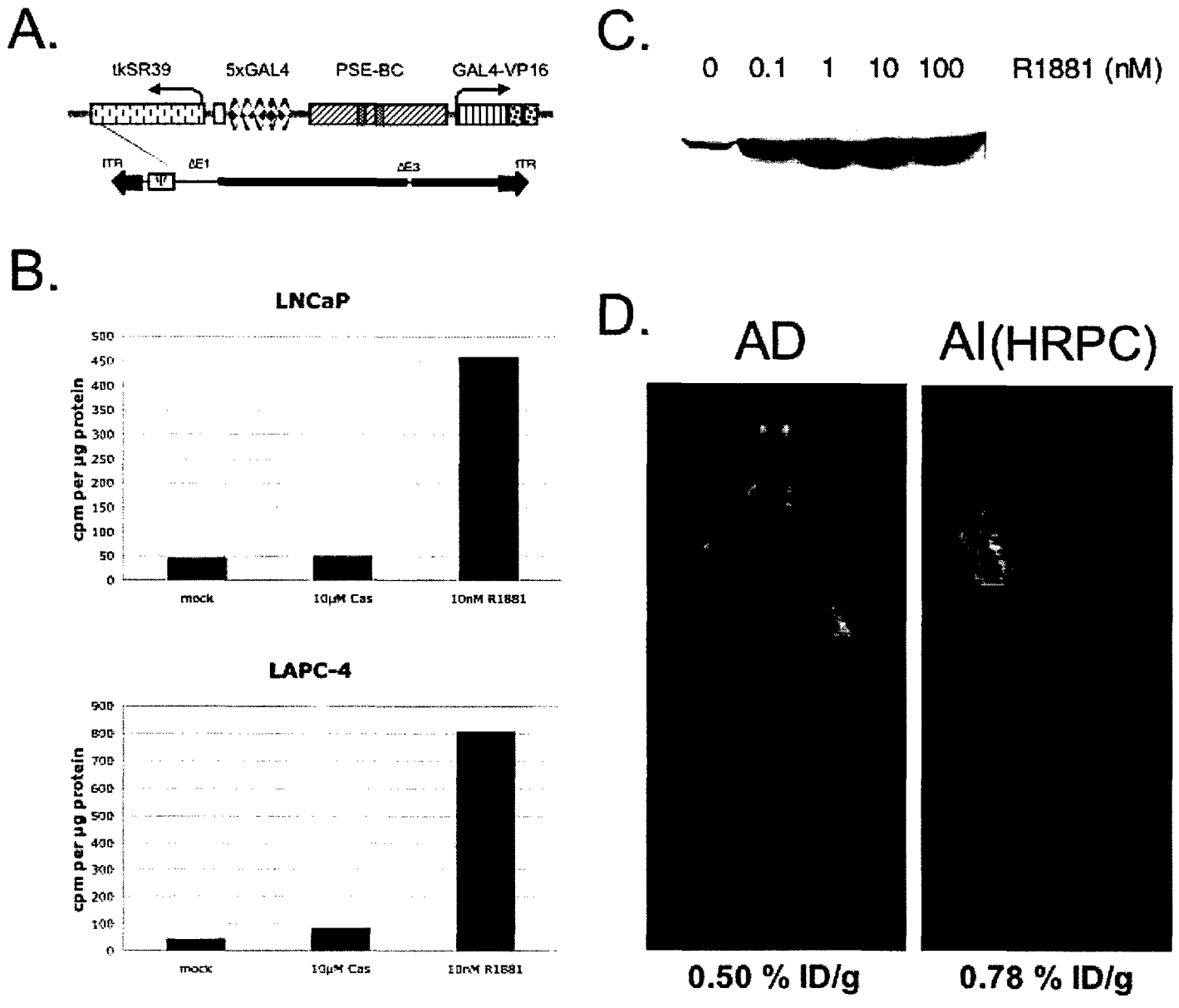
A.
tkSR39
5xGAL4
PSE-BC
GAL4-VP16
ITR
δE1
ΔE3
ITR
B.
LNCaP
cpm per µg protein
500
450
400
350
300
250
200
150
100
50
0
mock
10µM Cas
10nM R1881
LAPC-4
cpm per µg protein
900
800
700
600
500
400
300
200
100
0
mock
10µM Cas
10nM R1881
C.
0 0.1 1 10 100 R1881 (nM)
D.
AD
AI(HRPC)
0.50 % ID/g
0.78 % ID/g